Journal of Geography and Geology; Vol. 6, No. 3; 2014
ISSN 1916-9779 E-ISSN 1916-9787
Published by Canadian Center of Science and Education

Application of ERT and Aerial Photographs Techniques to Identify the Consequences of Sinkholes Hazards in Constructing Housing Complexes Sites over Karstic Carbonate Bedrock in Perak, Peninsular Malaysia

Riyadh R. Yassin[1], Ros Fatihah Muhammad[1], Samsudin Hj Taib[1] & Omer Al-Kouri[1]

[1] Department of Geology, Faculty of Science, University of Malaya, 50603 Kuala Lumpur, Malaysia

Correspondence: Riyadh R. Yassin, Department of Geology, Faculty of Science, University of Malaya, 50603 Kuala Lumpur, Malaysia. E-mail: riyadh.geophsea@gmail.com

Received: April 14, 2014 Accepted: May 16, 2014 Online Published: June 24, 2014

doi:10.5539/jgg.v6n3p55 URL: http://dx.doi.org/10.5539/jgg.v6n3p55

Abstract

The position and condition of carbonate bedrocks such as limestone or dolomite and its appearance are important for engineering construction sites such as buildings, housing complexes and road projects. In spite of the subsidence damage resulting from carbonate dissolution causing massive losses all over the world, the causes are well addressed in a few areas only. The application of a geophysical field survey and aerial photograph will be represented through identification techniques.

In this case study, a two-dimensional (2D) electrical resistivity tomography (ERT) survey was performed across two housing complex construction sites, north of Ipoh city, in the Perak state, Peninsular Malaysia, to image the subsurface and locate evidence for the near surface karstic features such as voids or cavities including sinkholes. Furthermore this survey was carried out to estimate the depth of the bedrock and to assess the reliability of the (ERT) electrical resistivity method whether it can identify such features or not.

Six resistivity traverses or profiles were conducted along the survey area at each of the two construction sites. The orientation, extension and the degree of inclination of those profiles are shown in the location map. The correct resistivity data was interpreted using res2dinv software. The interpretation of E R Tomography/ image sections revealed that many anomalies with very low resistivity and high conductivity extend along the project areas in these construction sites. Massive sinkhole has affected many sections of the project area in construction site #1. Thus it contains non-stiff clay and is saturated with water, rendering it less resistant to electrical currents (high conductivity). Enormous longitudinal channel pipe containing both stiff and sandy clay has affected many sections of project area in construction site #2. An assessment of the situation was surmised from the subsurface images. Subsequently, an estimation of the possibility of a collapse occurring in the near future due to the sinkhole was prepared.

This study also demonstrated that the high-resolution Electrical Resistivity Tomography (ERT) can be effectively applied to reflect and differentiate surficial soil, clay, weathered rocks, compact or intact rocks, and air-filled karstic voids or cavities. The appearance of many sinkholes in the area is mostly attributed to karstic activity. In accordance to the classification of the characteristics of morphological features of karstic ground conditions by Waltham and Fookes (2003), the karst level in construction site#1 found between profile 1 and profile 6 is an older or complex karst type KIV, while the karst level in construction site#2 found between profile 1 and profile 3 is a mature karst type KIII. Afterwards, the karst type changed over profile#4 to profile #6 to an older karst or complex karst type KIV.

The hazards of the sinkholes and other karst features such as, cavities and dissolution channel pipe can cause problems to the construction projects in the near future resulting to mismanagement during the initial phase of the projects, as the developers did not carry out prior geophysical technique and geological studies. Moreover, the borings within these karsts regions is incapable of providing sufficient subsurface data for analysis, and then might misrepresent the subsurface geological model, which might in turn lead to an additional cost for corrective design or an ad-hoc analysis.

Consequently, early engineering subsurface remediation techniques are needed to minimize the potential of geohazard of sinkholes and other karst features in these construction sites over karstic carbonate bedrock. Initially, it was considered to utilize the reverse graded filter technique to fill the huge sinkhole in construction site#1. Skin friction piles driven into the layers contained non-stiff materials (soil, clay, silt, sand). New chemical grouting techniques such as deep injection chemical grouting technique are utilized in construction site#2. Controlling of the surface and ground water drainages will be in force when work begins at these construction sites.

Keywords: ERT and aerial photographs, Identify consequences, Sinkhole Hazards, constructing housing complexes, karstic carbonate bedrock, Perak - peninsular Malaysia

1. Introduction

Sinkholes are the concern of construction sites which overlays Kinta karstic carbonate bedrocks such as dolomitic limestone or marbleized limestone in Ipoh causing construction delays and stability problems, which may amplify the increase in cost due to cracking of walls, building foundation collapse, road with pavement subsidence and cracking. These are only a few examples of the problems associated with sinkholes, karstic cavities and voids. Structural instabilities associated with these features can arise as a result of sudden collapse of the ground surface or as a less catastrophic but recurring drainage problem.

Within the karst regions, design and execution will be expensive regarding present and future structures. Besides, borings drilled within carbonate karst regions do not overlap areas of concern in the subsurface. Inappropriate and mismanaged borings cannot provide ample subsurface data for analysis and at the same time can also misrepresent the subsurface system which may lead additional cost for corrective design or additional analysis.

Rapid reconnaissance surveys using aerial photography and/or satellite images and surface geophysical survey techniques incorporated with a boring plan are the best obtainable options that can be used to aid in the suitable location of test borings to identify or distinguish the subsurface features related to karst development.

The 2D resistivity imaging technique was preferred for subsurface investigations instead of other geophysical techniques for its high contrast or disparity in resistivity values vis-à-vis the different types of sediments, such as carbonate rock and clay or soil, air or water in-filled cavity or voids, compared to the bordering or surrounding limestone bedrock.

These entire elements reflector reproduce the use of resistivity imaging technique to outline and delineate the boundary between bedrock and overburden. These entire elements reflector reproduce the use of resistivity imaging method that outlines and delineate the boundary between bedrocks and overburden. Moreover, this method is manageable with respect to time for small-scale projects in both pre and post-ability processing steps, rendering it the most appropriate for this type of investigations.

Electrical resistivity tomography surveys were functional at two constructions sites to the north of Ipoh city. Construction site #1 is located at Klebang Putra – Klebang Green and Construction site #2 is located at Medan Klebang Restu-Klebang Damai. Figure 1 highlights the locations of the studied construction sites in Kinta valley, north of Ipoh city, Perak, peninsular Malaysia.

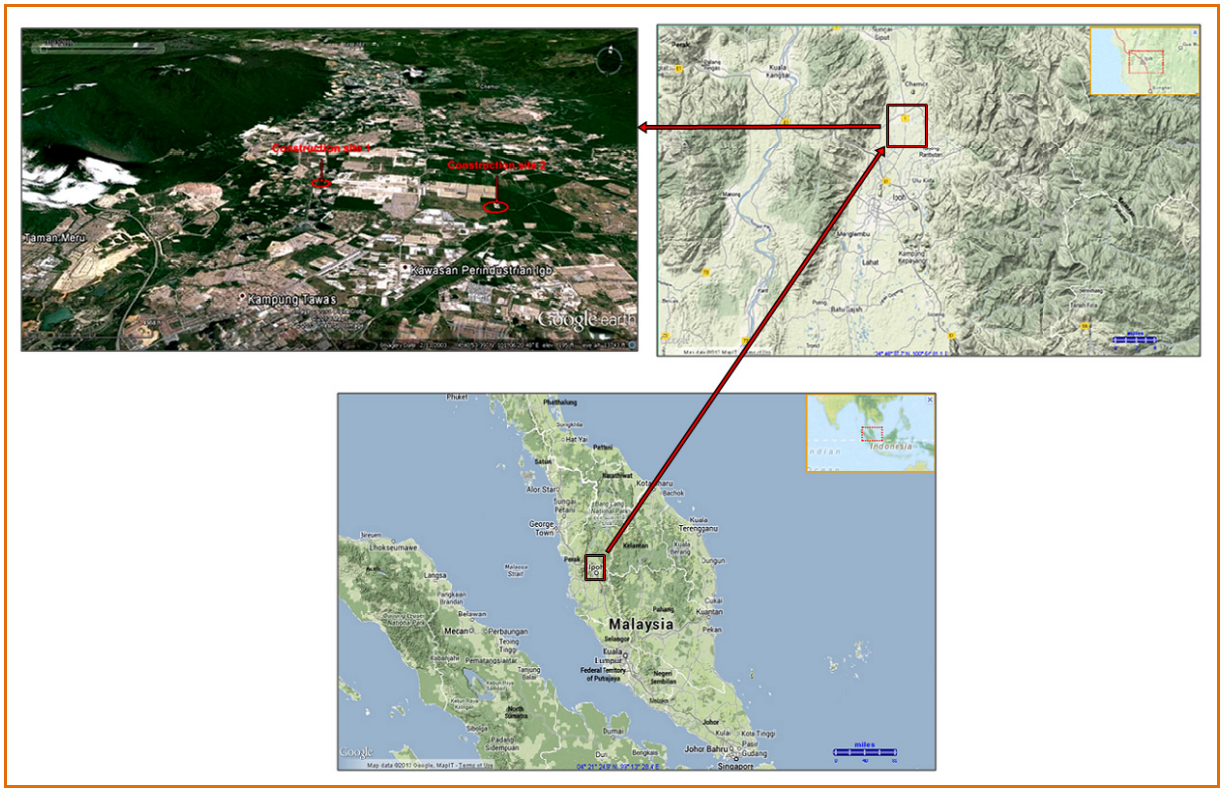

Figure 1. Google normal, terrain satellite images (2013) of Perak viewing the location of studied construction sites #1and #2, in Kinta valley, north Ipoh city, Perak state, Peninsular Malaysia

2. The Study Objective

The objective of this survey is to:

I. Figure out the subsurface to locate evidence for near surface karstic features (voids or cavities); including sinkholes in these construction sites over karstified carbonate bedrock.

II. Estimate the depth, shape and type of the sinkholes.

III. Understand the origin of these sinkholes.

IV. Find out whether clay or air-filled karstic voids or cavities are present in the subsurface.

V. Estimate the depth of the marbleized limestone bedrock.

VI. Produce the geological model to represent the study area.

VII. Evaluate the subsurface structure levels and extent that can result in potentially dangerous collapse or ground failures at construction sites that super-impose these features.

VIII. Identify subsurface conditions that might compromise the reliability of any proposed future work in these sites, for example, an inactive sinkhole in-filled with thick clay. Under-compacted clay could present a critical problem, as the clays could accumulate under load, resulting in leakages all the way down to the bedrock.

IX. The best solution methods frequently used in the plan to minimize the risk of problem areas in these construction sites.

3. Location of Study Area

3.1 Construction Site #1

Site #1 is situated at Klebang Putra – Klebang Green to the north of Ipoh city (Kinta Valley). It is situated at latitude N4°41'0.96"-N4°41'26.96", longitude E101º05'55.68"-E101º06'21.6" as shown in Figure 2. It is located to the north of the main series, and east of the Gunong Kledang Range or series o. The project plan estimating the constructing housing complex include 100 two floor linked houses, 50 bungalow houses and its facilities.

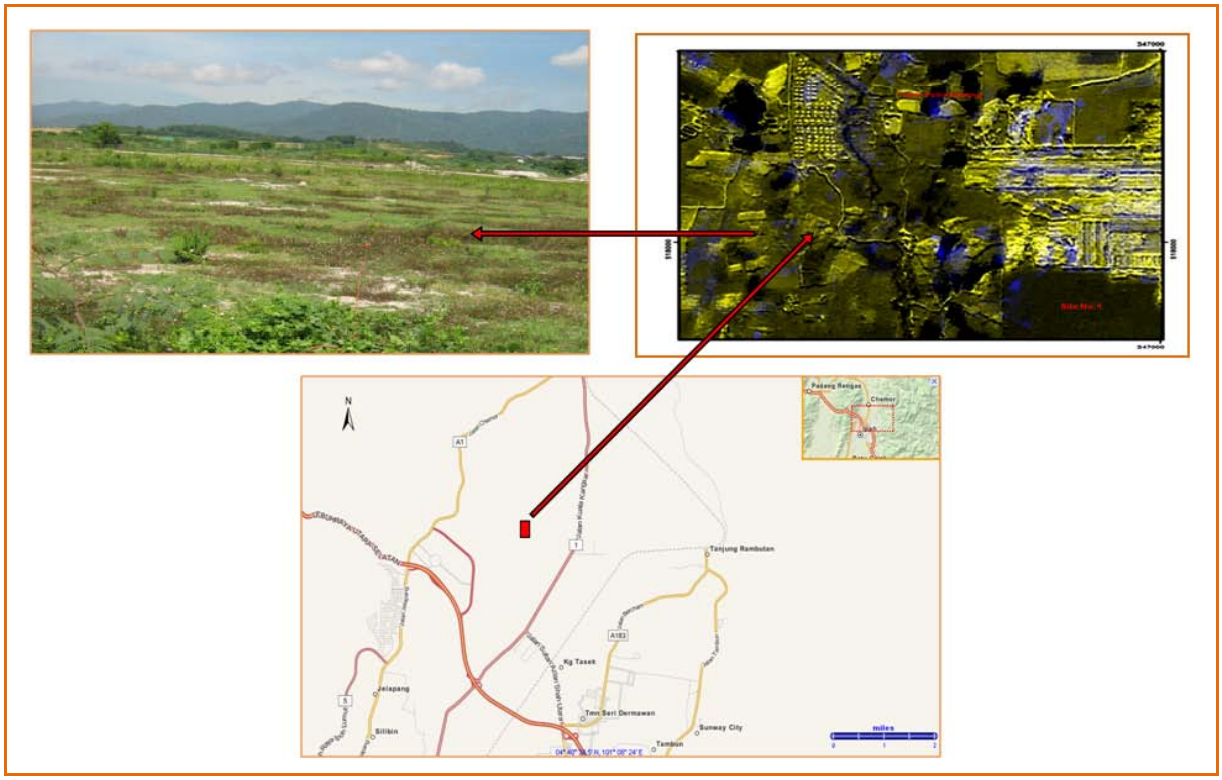

Figure 2. Location Map, Satellite images and land photograph viewing the location the study area in construction site #1

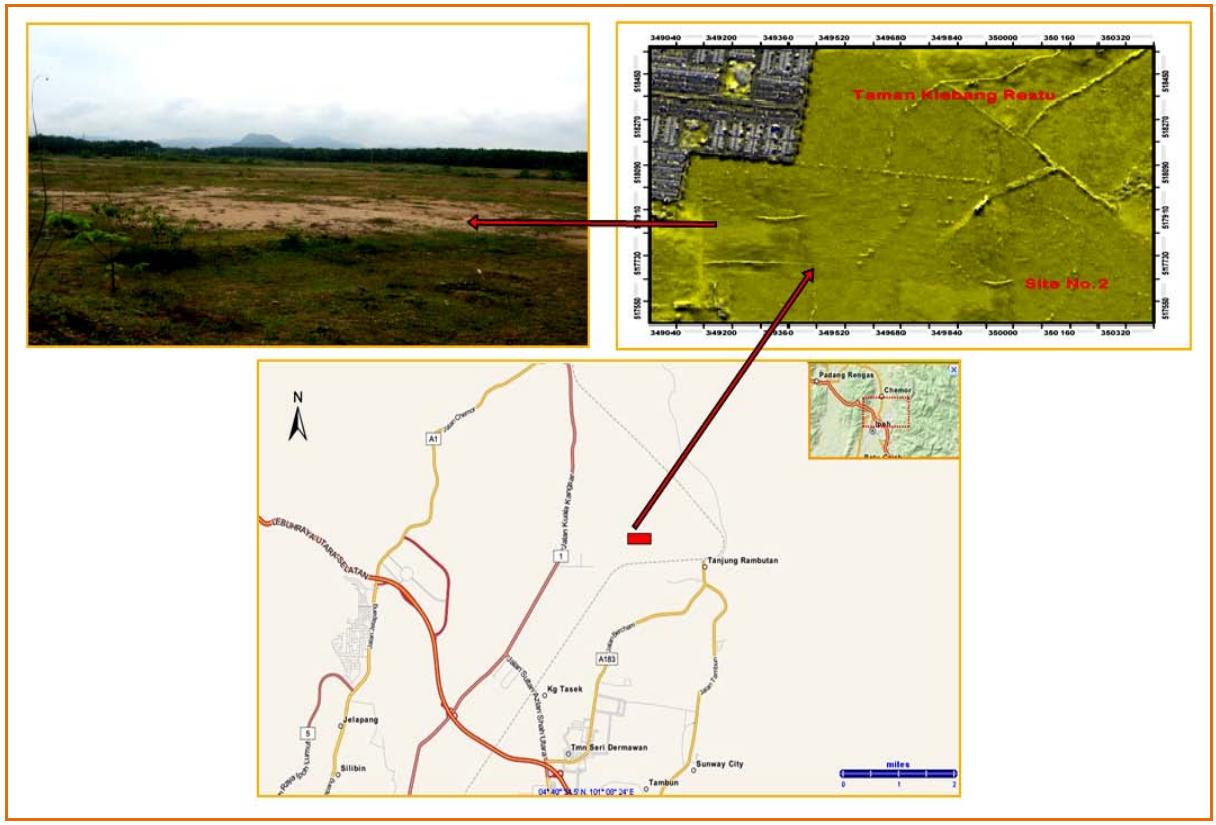

Figure 3. Location Map, Satellite images and land photograph viewing the location the study area in construction site #2

3.2 Construction Site #2

Site #2 is situated at Medan Klebang Restu- Klebang Damai to the north of Ipoh (Kinta Valley), positioned approximately at latitude N4°40'35.04"-N4°41'0.96", longitude E101º07'52.32"-E101º08'18.24", as shown in Figure 3. It is located to the west of the main Range or series of Cameron Highlands. The project plan to estimate the construction housing complex to include 150 two floor linked houses and its facilities.

4. Geology of the Study Area

The Kinta Valley is located in western Peninsular Malaysia, a V-shaped plain valley open to the south and flanking the granitic enormous uplands of the main series to the east and the Western or Kledang series to the west. The granite that forms these mountains has been dated to the Triassic age (Cobbing et al., 1992). The plain is enclosed by Tertiary to recent alluvial deposits of varying thickness layers over the entire expanse of Kinta Valley and beyond. Underlain by rugged and jagged subsurface of the Palaeozoic limestone platform. Rivers from the two highlands provide uninterrupted supply of allogenic water to the foot plain and consequently create wet and swampy conditions.

The marbleized limestone bed rock that sticks out above the enormous flood plain forming hills (mogote or tower karst) with steep-sided to vertical slopes. These hills are covered by a huge amount of vegetation. The outcrops of hills can be found widespread on the eastern part of the study area which is made up mostly of metamorphosed to marble of Silurian to Permian age. Only 30% of Kinta limestone occurs as limestone hills while the rest are subsurface karstic limestone (Muhammad, 2003). Studies using micro erosion meter gives the assessment of limestone deprivation rates for standing water, running and under sub-aerial condition and the values are 224 mm/ka, and 334 mm/ka and 369 mm/ka correspondingly (Muhammad & Yeap, 2002).

These hills are made up from the remnants of extensive limestone beds, which are part of the large Palaeozoic carbonate platform complexes that covered parts of South-East Asia. The Palaeozoic limestone outcrops are scattered intermittently throughout Peninsula Malaysia. The original limestone beds of Kinta Valley, presumed to be Carboniferous (Ingham & Bradford, 1960; Hutchinson, 2007) or possibly Permian in age (Fontaine & Ibrahim, 1995) have been severely eroded and karstified. Deposited more than 250 million years ago and buried to great depths, lithified and eventually brought to the surface by tectonic forces, presumably in the Mesozoic. The Palaeozoic limestone of the Kinta Valley was exposed to a humid tropical to equatorial climate for very long periods of time, which slowly dissolves the limestones. The hills are the only remaining visible part of the Palaeozoic limestone.

The limestone of Kinta Valley overlay extensive younger granite bodies, which affects the texture and composition of the limestone via contact metamorphism at the time of granite intrusion, originating from the Triassic age (Cobbing et al., 1992). Initial observations revealed that the degree of metamorphism of the limestone varies from hill to hill, from low (practically intact limestone) to high (limestone entirely turned to marble). Most of the Kinta Valley limestone has undergone contact metamorphism from Sungei Siput in the north to Tapah in the south. The less metamorphosed limestone is located in the northern part of Kinta Valley.

The lithology of the Kinta Valley consists of; the Kinta Limestone, granite of the Main series and Kledang series, other metasediment such as, schist and the Quaternary alluvial deposits. Kinta Limestone was named after Kinta Valley in Perak. Suntharalingam (1968) suggested that most of the study area is underlay by the Kinta limestone which shows an age range from Devonian to Permian. Lee (1971) believed that the age of the Kinta Limestone is Silurian to Middle Permian. The limestone in the study area is always calcitic, granular and homogeneous though some dolomite and mica do occur in some places. Table 1 below summarizes the stratigraphy of the area.

Table 1. Summarize the geology/stratigraphy of the Ipoh areas, after Gobbet (1961), Yin (1976)

No.	Age of units deposits	Type of units deposits in the study area
1	Quaternary	Alluvium (young and old)
2	Triassic	Granite & Allied rocks
3	Palaeozoic	Kinta limestone (dominant) Basal schist

The location of the construction sites under study in the Kinta valley were viewed in the Geological map in Figure 4 below.

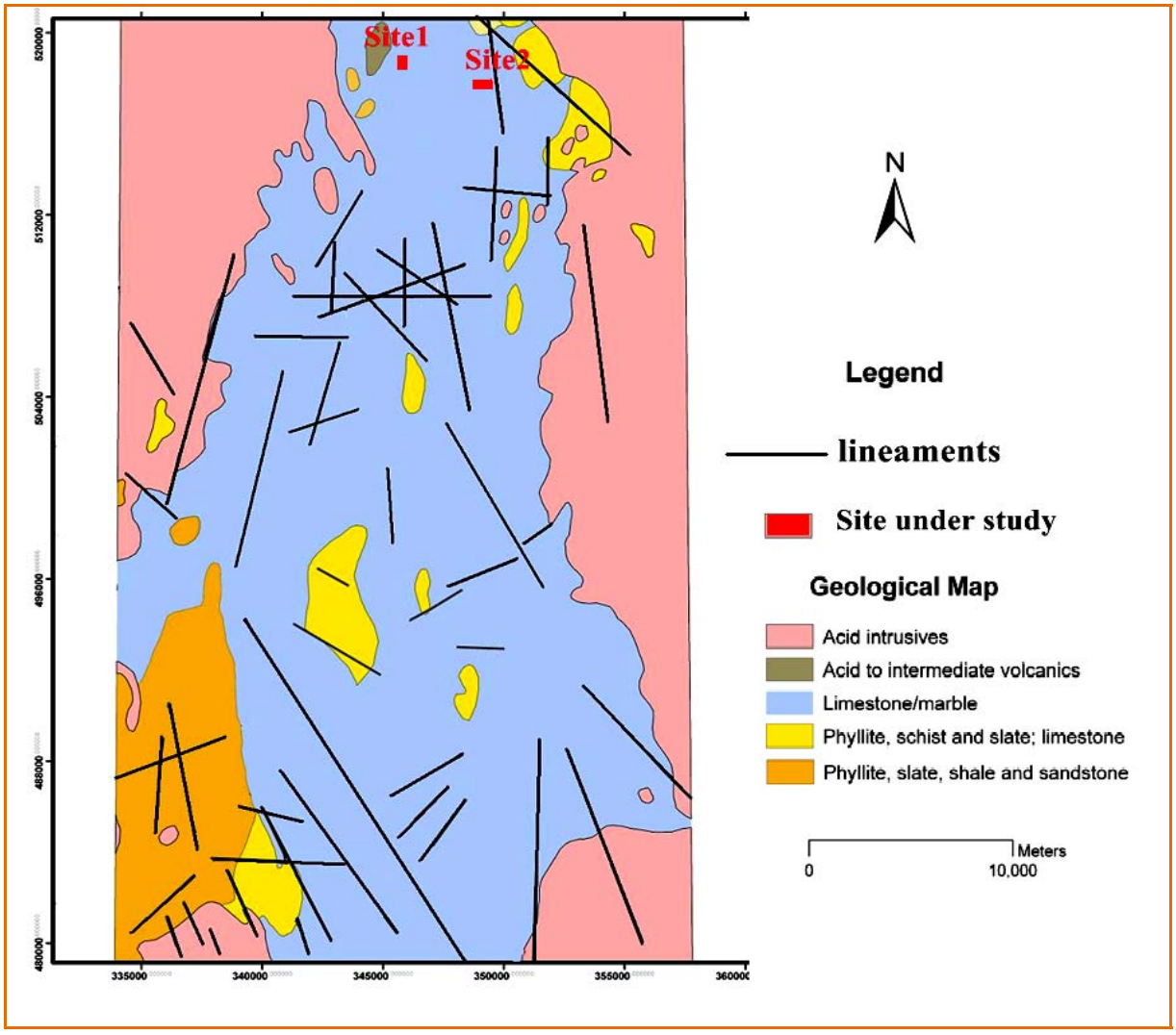

Figure 4. Geological map of Kinta valley viewing the location of construction sites under study north of Ipoh city, Perak state, peninsular Malaysia (Yassin, 2010)

5. Development of the Karst Phenomena in the Sungai Perak Basin (Kinta Valley)

Many geologists have suggested that major karstification is controlled by the structures in the areas where it occurs. The structural geology in the limestone of Kinta Valley are dominated by faults and folds oriented north-south, which results in a noticeable grain to the landscape, especially to the orientation of (mogotes) isolated, steep-sided, residual, and hills, which are composed of either limestone, marble or dolomite and surrounded by nearly flat alluvial plains in the central part of the valley. Vertical and sub-vertical joints and faults in the marble are its main lines of weakness. The subsurface karst is characterized by the formation of rounded top pinnacles and irregularly shaped sinkholes, which had previously been referred to as dolines.

Rainfall containing dissolved carbon dioxide results in a strong acid identified as carbonic acid (H_2CO_3). It will get more acidic as it filters through the side soil, as there is more carbon dioxide residing in the gaps in the soil – up to 100 times more than what is in the atmosphere. The author believes that the most imperative recent thought is the fact that enhanced rainfall and elevated acidity of the rain in the last few decades of the 20th and 21st century in Malaysia and other countries in South East Asia are due to the dramatic increase in the amount of liquefied carbon dioxide.

These are mostly caused by volcanic and tectonic activity in the Pacific fire ring, with volcanoes in the Philippines such as Bulusan and Mayon volcanoes in the south east of Manila. In Indonesia such as the Kelud volcano located in East Java, Mount Sinabung volcano in North Sumatra, Mount Merapi volcano located on the border between Central Java and Yogyakarta, Indonesia, being the most active. A spectacular submarine

volcanic eruption spews out huge columns of ash, smoke, gases and vapours thousands of feet into the Pacific Ocean's sky. Land clearing activities such as those practiced by Indonesia on a large scale also results in the emission of large volumes of pollutants into the atmosphere. Vehicular and factory emissions are also significant contributors to air pollution. All of these events have a large impact on the development and quick dissolving process of carbonate rocks.

The authors also believe that most of the biggest cave and channels in the limestone of Kinta valley are due to the reaction of sulfuric acid (H_2SO_4) with carbonate rocks, and can also be one of the corrosion factors in karst formation; this mechanism may also play a role, as O_2-rich surface, rain water, surface water seep into the ground and carries oxygen which reacts with sulphide, which are present with Cassiterite into the ground surface of the Kinta valley area. The oxidation of sulphide leads to the formation of sulfuric acid. Sulfuric acid then reacts with calcium carbonate, causing an increased erosion within the limestone's formation. The cover layers of alluvial deposits over marbleized limestone of Kinta valley contain soil-piping or channel features. The Tin (Cassiterite) accumulates in this alluvial channels or pipes, having been washed down from the granite ranges and carried by rivers as previously mentioned, which contain sulphur in its chemical deposits, having a large impact on the development and quick dissolving process of carbonate rocks.

6. Sinkhole Hazards

Sinkholes are the main crux of the geohazard issue in a limestone formation due to natural erosion processes. Sinkholes mostly were created on soluble carbonate rocks (limestone, dolomite, dolomitic limestone and marbleized limestone). Sinkholes are developed at both the surface and subsurface due to the dissolution related with the difference in composition and associated processes and posed many problems, which are classified by Waltham and Fookes (2003), into six types. Will present the type shown in the study area including, the Dissolution sinkholes which are formed by slow dissolutional processes. They are normal features in karst region that have developed over geological timescales. As an old feature it maybe reaches about 1000 m across and 10 m deep. The other type is a Collapse sinkholes which are formed due to the failure and collapse of the limestone roof over a large cavern or over a group of smaller caves. Subsidence sinkholes (both dropout and suffosion) that formed in soil cover within karst regions are created by the rapid failures of soil due to the downward percolation of water and many occur during heavy rainfall events, (Hyatt & Jacobs, 1996) which are the major sinkholes hazards to civil engineering works. The most foundation problems occur where soils 2 - 10 m thick overlay a fissured rock head. Occasional large failures are known in soils 30 - 50 m thick (Jammal, 1986).

In the Kinta Valley, Perak, the sinkholes formed within the region which extended from Tapah till Kuala Kangsar included two zones. The first trending zone from the south to the north-northeast, while the other zone trending from the south to the north-northwest of the valley. Distributions of sinkholes are mostly located in the southern part of the western belt of limestone hills and as east-west line across Ipoh. Therefore, sinkhole development is more common in the pure limestone with over 95% $CaCO_3$ content while the more dolomitized karst areas with about 40% $MgCO_3$ content are less level to the sinkhole development (Teh et al., 1998).

The natural of Karst features in the carbonate bedrock such as pinnacle topography; cavities and linear trenches all contribute or provide the geologic settings for the development of sinkholes. Man-made factors or activities such as changing the groundwater level by pumping for watering the farm and deep excavations to open-cast mining can generate the formation of sinkholes, occurrence of rock fall, soil erosion and subsidence. Also, excavations of the lands, removing the trees for constructions projects works. Therefore, it is reasonable that sinkhole problems have become the common interest not only for geologists and engineers, but also city planners and even enterprise or project managers.

6.1 Evolution of Sinkhole in the Study Area

The solubility of limestone in water and weak acid solutions leads to karst landscapes. The study region overlaying marbleized limestone bedrock in the Kinta Valley region tend to have fewer visible surface water sources of ponds and streams and can easily drain downward through joints and fractures in the marbleized limestone bedrock. Sinkholes can occur due to many reasons; however, it still requires more studies to provide sufficient results to conclude the relationship between sinkholes and subsidence with the following factors.

6.1.1 Running of Heavy Rain Water

The primary source of sinkholes or subsidence in the study area is the dissolution of marbleized limestone bedrock in the Kinta Valley region by acidic waters. Rain water which absorbs the carbonic acid solution by percolating through the natural features, which is known technically as joints, fractures or faults within the bedrock, and was slowly, dissolving it. Through geologic time, dissolution along these zones of weaknesses has

resulted in the formation of the cavities within the bedrock, and the soil immediately above these cavities would migrate or collapse down.

If the groundwater table is high, the hydrostatic pressure on the roof of the void prevents the collapse of the soil into the cavities. However, if the groundwater table there is lowering down, a rapid collapse to the soil will happen here leading to the formation of a sinkhole. Studies have shown that rapid fluctuation changes in the elevation of the water table can lead to the formation of sinkholes. There are a number of reasons for the rapid fluctuation. One of the immediate causes of sinkhole formation is:

First, the heavy rains, the rapid infiltration resulting from heavy rainstorms can often generate sinkholes and remove the soil and the sand particles from the surface and drain it to the ground water.

Second, the extended period of water lack and water withdrawal for use and excess water withdrawal from the area will lower the water pressure in the limestone bedrock which, in turn, will increase the water seepage from the overlaying soil into the limestone bedrock. This increased seepage will wash the soil down into cavities and activates the surface collapsed.

Third, the human activities often cause increased deformation into the soil and bedrock. Occasionally, construction activities disturb or overload the roof of a void leading to a sudden collapse of the roof. Construction or mining activities that intercept the drainage from a large area and concentrate the information of this drainage at the one spot may also trigger a sinkhole formation.

6.1.2 Earthquake and Subsidence

Fatiha, AL-Kouri and Yassin (2010) carried out site investigations in kampong Jeram, northwest of Kampar city, Kinta Valley, which showed that there are different levels of damages in the mining area. In addition, the image processing and statistical analysis have shown that the number of sinkholes had increased after the tsunami which took place on 26 December 2004, with up to more than 10 m in diameter. A recent spate of sinkholes, totaling about 40 in number, appeared in an area south of Ipoh city within the Kinta Valley soon after the major earthquake of Sumatra on 26th December 2004.

According to Chow (2005), these sinkholes were correlated with the tremors from the Sumatran earthquake. However, the geologic conditions where these sinkholes were developed, namely limestone bedrock overlay by mostly sandy mine tailings, were said to have a high potential for the formation of sinkholes and the earthquake vibration supplied the triggering factor to initiate their development. It was reported that the same earthquake also triggered a spate of sinkholes in Thailand (Chow, 2005). The geophysical survey in the area according to Yassin (2012) showed many subsurface cavities and sinkholes which were not connected to the surface. This made the area dangerous to be used and for living in by farmers due to any sudden collapse in the near futures.

6.1.3 Human Influence

Sinkholes are of two types, natural and induced which are accelerated or caused by humans. Most of the induced or accelerated sinkholes caused by humans in the construction site are due to the alteration of surface drainage over unconsolidated deposits resting on the openings in the top of bedrocks. The collapse mechanisms include loading, saturation, and piping. The decline in the water level is due to ground-water withdrawals causing a loss of buoyant support, an increase in velocity of water movement, water-level fluctuations, and an induced recharge. These types of sinkholes usually happen in places that were otherwise unlikely to happen. The sudden development of both types of sinkholes results from the collapsed of the roof of a cavity or cavern in rock or from the downward migration of unconsolidated deposits into solutionally enlarged openings in the top of bedrock (Newton, 1987).

Soil conventionally is a material used in burial sites, building foundations and as construction material for buildings. The use or soil removal may also cause unexpected surface level changes that lead to sinkhole developments. Also, the heavy loads of construction projects on the surface of land, such as large building structures may lead to unexpected sinkholes. Disturbances in the surface soil, such as digging, drilling and injections of water in the ground may cause sinkholes to form (Kochanov & William, 1999; Newton, 1987).

6.1.4 Vibration from Traffic

Heavy vehicle passage along the roads and highways in Perak can cause the ground to vibrate. These vibrations will be more effectual if the road is very busy. The consequence of this is that the ground surface will lose its strength in response to strong ground shaking. Therefore, at least 24 subsidences and sinkholes have been found in the areas close or near to the express high way of Gopeng to Ipoh and from Ipoh to Kuala Kangsar. These sinkholes were most probably developed due to the frequent traffic crowd (Kochanov & William, 1999).

6.1.5 Weather Patterns

Seasonal changes, such as the changes that occur from cold and hot weather, may cause sinkholes due to the fluctuations in the groundwater-level. Extreme precipitation is another cause of sinkholes due to the unexpected increase in water, such as flooding, or decrease in water, such as a drought (Sinclair, 1982; Newton, 1987).

6.1.6 Water Quality

Water samples taken from (40) forty numbers of sinkholes and surface water pools were collected and analysed. The results of these analyses showed that an extensive change in the chemistry of these waters have occurred under natural conditions. The dissolution processes of the dissolved material are exceedingly high. The results for the Total Dissolved Solid (TDS) and pH of the water samples are as follows:

I. PH reading which basically is a measure of the acidity or basicity of water. The pH value reading in the study area ranges between 5.25, 5.49, 6.65 and 6.77. Pure water with a pH close to 7.0 at 25 ^{o}C is Neutral. Water with a pH less than 7 is acidic and with a pH greater than 7 is basic or alkaline.

II. Total Dissolved Solid (TDS) reading ranges from (85.4, 125.7, 185.8 to 249 mg/L). The low total dissolved solid value will cause the resistivity value to be high. This is due to the lack of ions in some materials as electric conductor.

III. The results of these analyses showed the sodium content varying from 2.64 to 2.65 mg/L. and chloride content varying from 2.70 to 17 mg/L.

IV. The analysis shows that extremely high calcium content ranging between 48.2, 65.4 and 73.8 mg/L.

7. Identification Technique Performed Across the Study Areas

7.1 Identification of Sinkholes and Subsidence Areas by Applying Geophysical Technique

The assortment and application of geophysical techniques intended to reduce the risk of sinkhole formation generally require the detection of existing sinkholes and the explanation of the areas where unique sinkholes are most likely to occur in the future. It is also imperative to gather information regarding the size and the frequency of the sinkhole events, subsidence mechanisms, and rates. However, it is usually a tedious task to identify the areas affected by carbonate dissolution subsidence. Sinkholes are usually enclosed by human activities, such as filling and development, or natural attrition processes which may well eradicate them.

Generally, sinkholes may have a very fine geomorphic appearance, as the collapse produced by the underground processes may have yet to reach the ground surface. Many sources of surface and subsurface information need to be examined in order to gather sufficient data regarding the past and existing subsidence movement in the study area. In order to partially address these difficulties, the geophysical examination techniques can be used to detect the changes in the physical properties and the anomalies of the ground that is connected with air-filled, water-filled or sediment-filled cavities, breccia pipes, subsidence of structures ravel zones, syncline hang down, down thrown blocks, irregularity of rock head topography and covered sinkholes. Major characteristics of the ambiguities must be acknowledged for certain interfering methods such as excavating trenches, borehole drilling or applying of borehole probing.

There are a multitude of methods whose applicability and fitness depends largely on the investments available, type of necessary deposits, geological situation uncovered, the over covering or inter layers of the karsts, the topography of the area and the probable type of structures dissolution, the estimated type of structures subsidence, existence of interfere factors such as man-made services, and the required penetration and declaration. Sinkhole activity has become obvious in developed areas, especially via the deformation of roadways and buildings, intermittent services, and other formation. Applying geophysical approaches for mapping the subsidence destruction, information on the spatial allocation of the subsidence can be gained, and major natural and human factors that control the dissolution and subsidence processes may also be conditional. Devastation of buildings can also be recorded on the performance evidence sheets for it to be converted and supplied to a GIS and database system.

The best option is to apply two or more geophysical techniques, and compare the results to each other. It is wise to apply the geophysical examination techniques on the sites prior to drilling as one of the phased sequences of investigation. The area with aberrations and the normal areas unfilled of aberrations are recognised delineated, and planned for construction projects. The evaluation of geophysical techniques used in karst areas have been presented by Hoover and Saunders (2000) and Waltham and Fookes (2003). A number of previous geophysical studies in the karst areas apply the (ERT) technique to map the bedrock surface (Zhou, Beck, & Stephenson, 2000), a site in southern Indiana, where limestone is covered by about 9 m of clayey soils. Forty-nine profiles

were created over an area of approximately 42,037 m^2. The reliability of the ERT technique was evaluated by comparing the previous drilling section, with the interpreted ERT section from pairs of transects where they crossed each other. To identify the depth of mud-filled void and its extension, William, Jonathan, Philip, Kaufmann, and Bradley (2002) conducted geophysical surveys at a site on the Oak Ridge Reservation (ORR), Tennessee, USA. The data suggested that an optimal scheme for detailed karst mapping might consist of multi electrode resistivity surveying, followed by the joint inversion of gravity and seismic travel time data. The resistivity results could be used to produce an initial model for the seismic and gravity inversions. To identify buried sinkholes and other karst features in the zone of karst terrain, Kachentra and Tanad (2007) applied 2D and 3D resistivity imaging resistivity (ERT) survey at the Ban Pakjam in Huaiyod district, Trung province, southern Thailand. The 2D resistivity surveys clearly showed the central depression, as well as resistivity contrasts between the cover sediments, delineating the in-filled sinkholes, underlying weathered bedrock, and map the locations of sinkholes in this covered karst terrain

7.2 Identifying Sinkholes by Employing Aerial Photographs and Satellite Images Technique

Large-scale colour stereoscopic aerial photographs are very helpful in identifying sinkholes. The key limitation of aerial photographs and satellite images is that, depending on the scale and explanation of the images, it may not be feasible to pinpoint small or shallow sinkholes. The location of construction site #1 and site #2 was presented in the satellite spot image map (2010) shown in Figure 5.

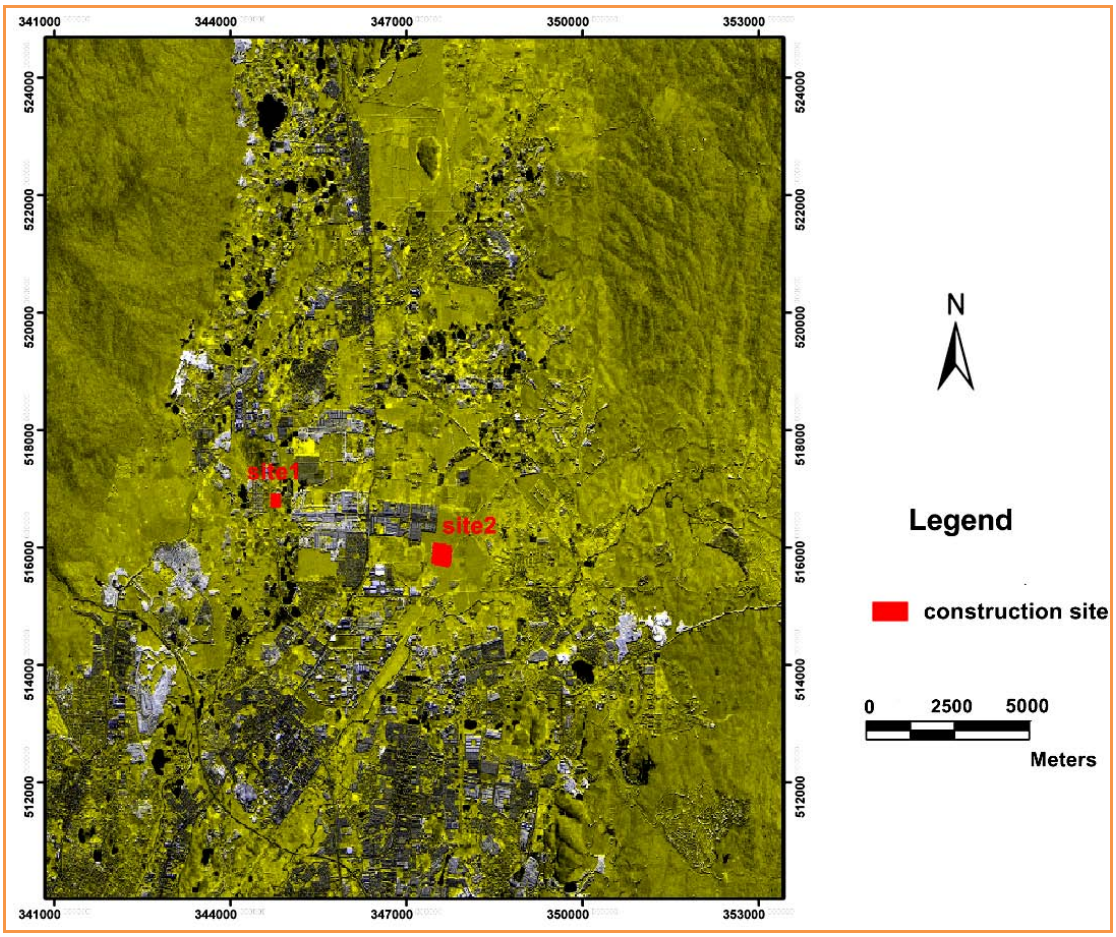

Figure 5. Satellite spot image (2010) presenting the location of construction site #1and construction site #2 in Klebang Raya north of Ipoh city (Kinta Valley)

Old aerial photographs are usually very helpful in detecting sinkholes that are enclosed by buildings or man-made structures. The thorough elucidation of photographs taken on different dates allows the chronology of freshly formed sinkholes to be inhibited. The interpretations help to gain minimum estimates of the possibility of sinkhole

occurrences, and permit the study of the spatial-temporal allocated patterns of the subsidence phenomena. The usage of low sun-angle photographs with apparent shadows emphasizes subtle topographic features.

The more advance technique is the investigation of airborne and satellite multi-spectral and thermal images, which may be used to distinguish the surface terrain patterns and acquire variations in moisture, vegetation, colours, and heat related to subsidence areas and sinkholes. In this current work, usage of satellite images of Perak is on the scale 1/5000 of year (2008). Additionally, the Global Position System (GPS) and Geographic Information System (GIS) technologies have immensely improved examinations. The common methods of mapping land and utilizing changes are typically high in cost and low in precision. The remote sensing provides updated information on land by using these methods. Natural events and human factors can also be observed by using current and archived distantly sensed data. The Five layers spot images of Perak state (2010) which presented the location of construction site #1, site #2 and site #3 north of Ipoh city (Kinta valley) are shown in Figure 6.

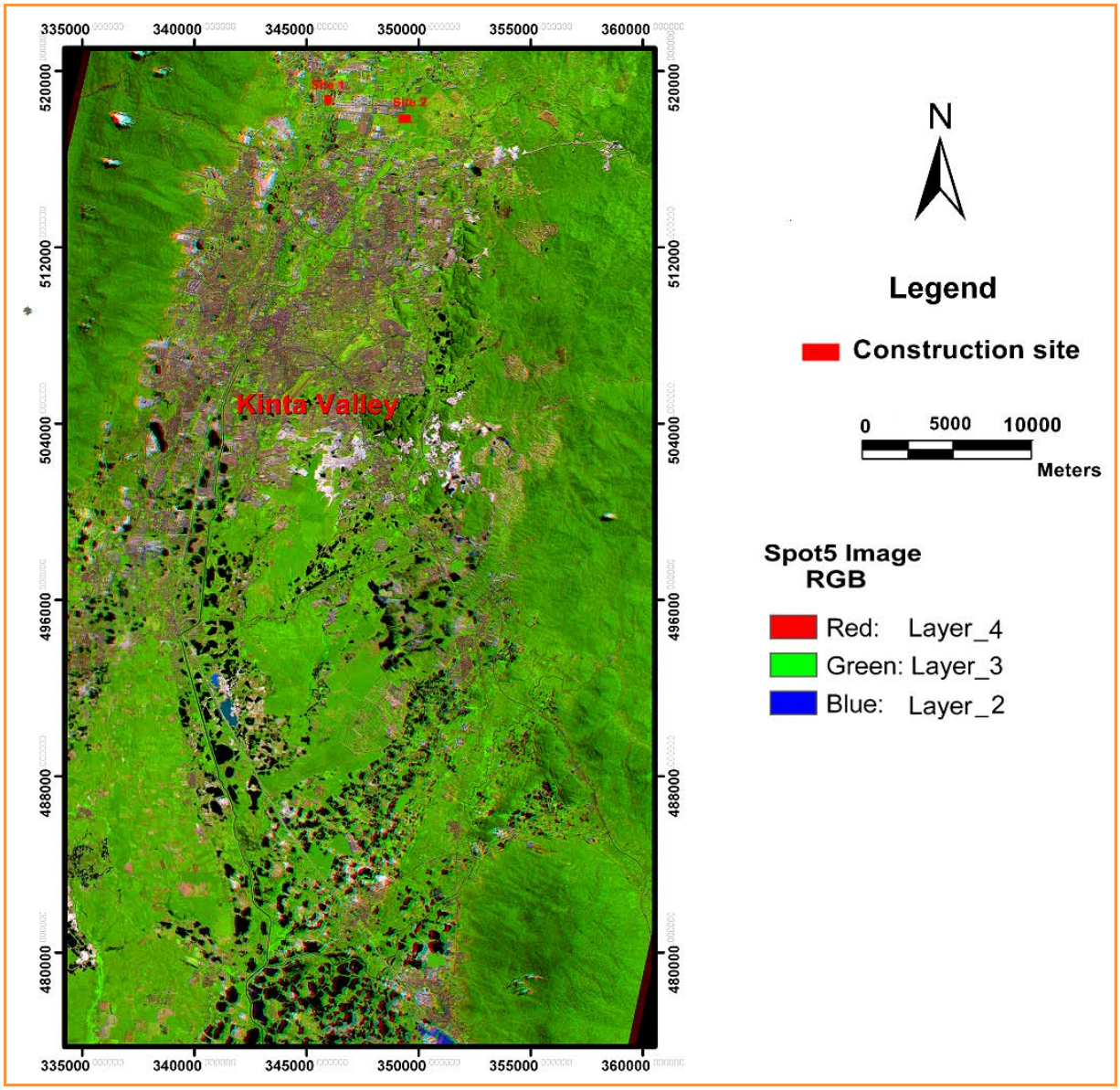

Figure 6. Five layers spot images of Perak state (2010) presenting the extension of (Kinta valley) and the location of construction site #1and construction site #2 , north of Ipoh city (Kinta valley), Perak

An interpretation of the aerial photographs of the study area and its surroundings to determine the fracture system, topography, and drainage pattern was conducted. These old aerial photographs were operational in 1965 under the Colombo Plan, possessing a scale of about 1:25,000. Table 2 shows the list of aerial photographs used in this study. The technique used for this aerial photographic interpretation of the karstic features are limestone isolated residual hills (mogotes) and the cliffs, and also the lineaments, forests, and plantations. The significance of the karstic features and their possible origin in relation to the geological features are concluded as well. Also, the interpretation showed that the orientation of lineaments from the Main Range and Kledang Range is far from irregular, but shows the dominant strike of northwest to Southeast, with a subsidiary set striking east-northeast to west-southwest. It was concluded that these lineaments were also observed to be clearly cutting the marbleized limestone of Kinta Valley and the hills above it. Figure 3 shows the direction of the lineament in the study area that are taken from the aerial photographs, satellite images, and setting on geological maps. The drainage in this study area is rather straight and angular, and aerial photographs show that stream courses are controlled by the direction of lineaments (joints, fractures and fault systems) in the marbleized bedrock. In addition, the aerial photographs show that the area of construction site #1 was a swamp area with bushes. The aerial photographs also show that the area of construction site #2 and site #3 were covered with forest, and some parts with oil palm plantations. Furthermore, the satellite images' show that part of the forest in site #1 were removed for the construction project. Moreover, it was determined that isolated residual limestone hills were distributed in the south and south west of construction sites #2.

Table 2. Presenting the list of aerial photographs which employed in this study

Location	Roll no.	Line no.	Print no.
Ipoh	C-12-A	L32N	20-30
	C-6	L31N	20-55
	C-5	L30S	80-90
	C-5	L29S	120-125

8. Reconnaissance Field Surveys

Direct ground inspections in the two construction sites resulted in the discovery of sinkholes that were not visible in the aerial photographs and satellite images due to many factors. For example, the area may be enclosed by vegetation, sinkholes of definite size, or their depth is too small to be detected. The recorded model is used for the explanation of each sinkhole, including a diagram of the sinkhole and its access geometry, the covering features with the district and the coordinates, orientation, dimensions, age, continuation degree, vegetation and symbols of volatility as cracks, scarps or pipes. These features supply information on the activity and the periods of the sinkholes, and act as indicators of plausible location of future sinkholes in proximity to human structures and other observations. The existence of the features such as muddy areas, or the expansion of vegetation and holes crammed with materials may help detect shallow subsidence depressions. Generally, the application of geophysical surveys is desired to determine whether these irregular characteristics are interrelated to sinkholes.

The ground inspection at site#1 reveals no sinkhole. On the other hand, aerial photographs of the area imply that it is made up of old swamps, which might contain sinkholes on its subsurface. More than four big black spots were recognized in aerial photographs, three of them circular to semi circular in shape, while the others possess an extended shape. However, due to human activity and excavating work being done there which was an ex–mining area, most of these features were packed with sand and other material. Among them, three areas with deposits of grey swamp clay in circular shapes were acknowledged. The clay seems to sink down due to numerous factors, which will be explained shortly. Figure 7 shows land photographs and the positions of three big black spots in the aerial photographs, which might include sinkholes under the depositional of gray swampy clay construction site #1.

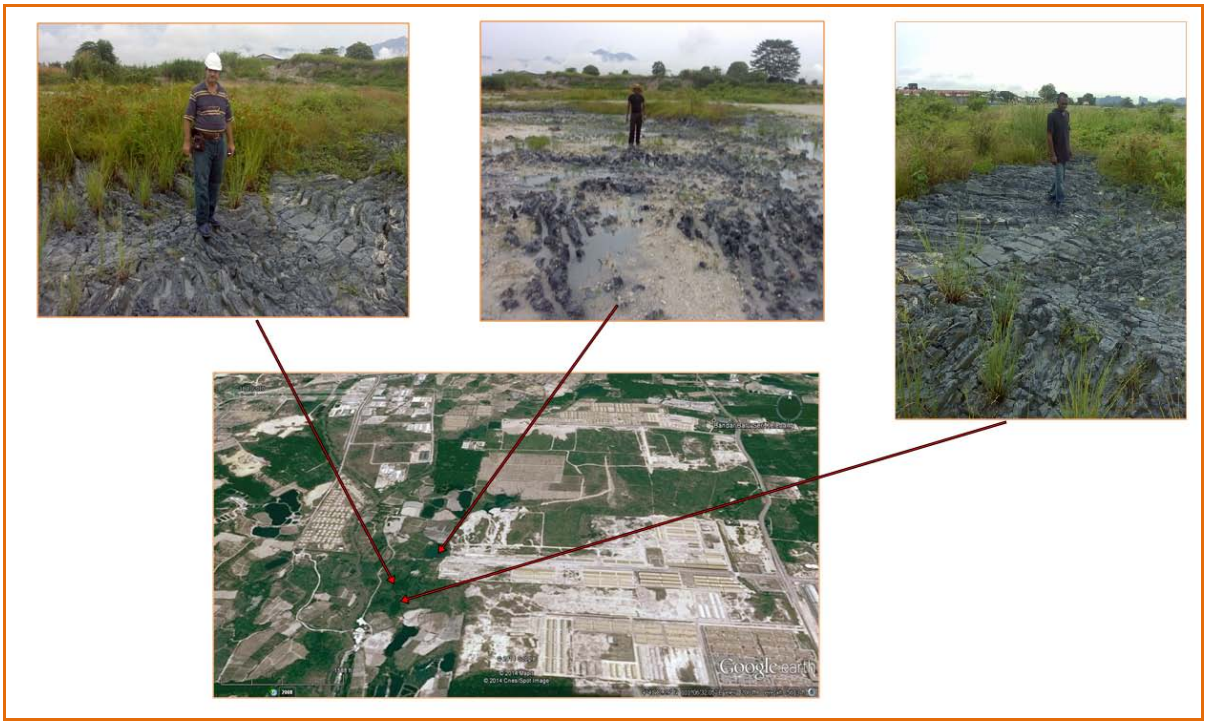

Figure 7. Land Photographs viewing several positions that recognized aerial photographs and satellite image (2008) in construction site #1, which was identified as the depositional of gray swamps clay

This area is identified and demonstrated as an area that might include a medium to large sinkhole, extended in the subsurface along this site of visually uncertain depth. This might point to the presence of clay or water in-filled karstic sinkhole or cavities that could compromise the probity of this site.

During the ground inspection at site #2, two sinkholes were discovered, but not recognized in aerial photographs and satellite images, as adjacent small plants have enclosed it. One of these sinkholes has a diameter of ~7 m – 10 m., water in-filled, of visually undetermined depth, are recognized and proven as a sinkhole with a narrow showing throat, positioned in the south west flank of this site. The other sinkhole has a diameter of ~35 m – 40 m, positioned in the north east side of this site, was in-filled with wet clay and other material of sediments due to karst activity, raised a question that this sinkhole might be linked in the subsurface to one or more of the large tabular conduits or channels, and the presence of cavities or voids of undetermined depth. Clay, or air in-filled karstic sinkhole or cavities were present, which could compromise the veracity of this site. The south section of this site is littered with soil cover collapses. The sinkholes that were identified as water in-fill or empty and some covered with vegetation were determined as small and narrow in construction site #2 viewing in Figure 8.

Figure 8. Land Photographs viewing a number of sinkholes that identified as water in-fill, empty and covered with vegetation were determined as small and narrow in construction site #2

9. Field Survey Technique

9.1 Instrumentation and Measurement Procedure

The survey was conducted using an instrument, type SAS1000 resistivity meter viewing in Figure 9, which has an inherent microprocessor that automatically selects the appropriate four electrodes for each measurement.

The two dimensional (2D) - electrical imaging/tomography surveys are typically carried out by employing a large number of electrodes; 41, 61 and 81 electrodes along a straight line, coupled to a multi-core cable, (Griffiths & Barker, 1993) commonly at a constant spacing of 5 m or 10 m between the adjoining electrodes. When the succeeding measurements were taken, they were configured in a Wenner array and other survey parameters, such as the electrical current is usually converted into a text file, which can be read by a computer program. After reading the control file, the computer program then automatically detects the suitable electrodes for each quantity. A laptop computer was utilised to set the RES2DINV inversion software for the purpose of developing the resistivity model.

In a distinctive survey, most of the fieldwork involves laying out the cables and electrodes. After doing that, the measurements are taken automatically and stocked into the computer. This resistivity procedure usually gives a better grouping of spatial resolution and depth of study in karst terrain than any other geophysical technique.

Figure 9. Viewing the instrument type SAS1000 applied in geophysical survey technique

9.2 Data Collection

Electrical resistivity tomography (ERT) was used to image the subsurface. The electrical resistivity data, was composed along two dimensional (2-D) electrical resistivity profiles, which were functional above and in proximity underneath, adjoining active and non-active sinkholes at two construction sites.

9.2.1 Data Collection in Construction Site #1 (Klebang Putra)

Six electrical resistivity traverses or profiles, Profile-1 to Profile-6, were controlled over and along the survey area in site #1. The direction of these profiles in (N90º W), and the level of those lines are shown in the location map, illustrated in Figure 10. The electrical resistivity data accumulated along the two dimensional (2-D) electrical resistivity profiles were determined to be in excess of, or beneath the sinkhole, using a 41-channel array in the Wenner configuration. The length of each profile was 200 m, with an electrode spacing of 5 m, on average, spaced at 25 m between each profile. The total length of all profiles in this site was 1200 m, covering an area of 30000 m^2; 190 data points were composed for each (41-electrode) in one profile, and on average, about 1140 data were composed for a total six profiles in this site.

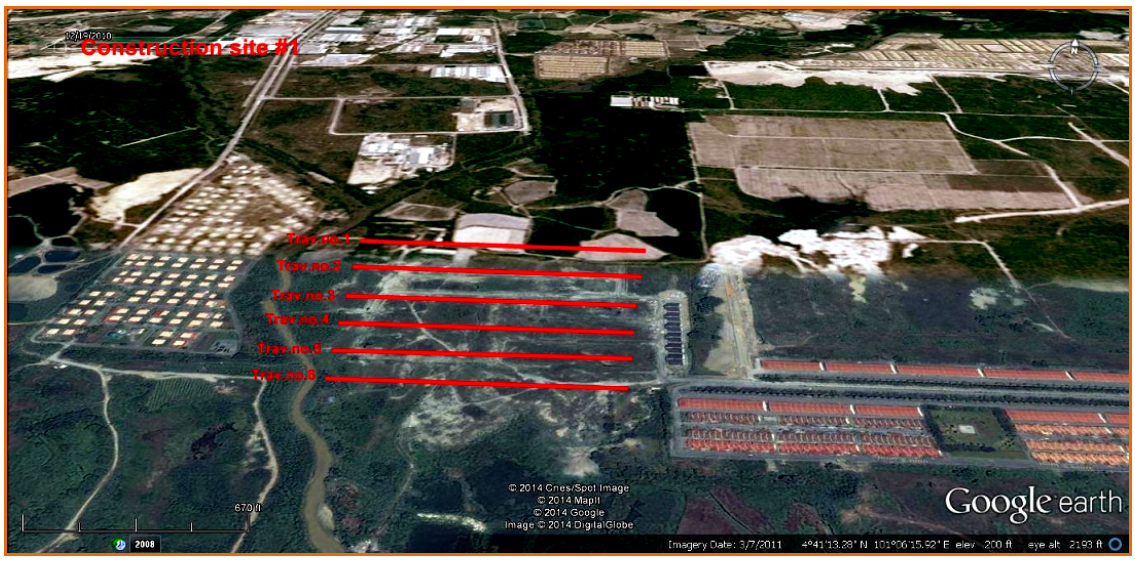

Figure 10. Google earth satellite images (2011) viewing the location of resistivity profiles in construction site #1

9.2.2 Data Collection In Construction Site #2 (Medan Klebang Restu)

Six electrical resistivity traverses or profiles, Profile-1 to Profile-6, were conducted over and along the survey area in site#2. The directions of these profiles are in (N80º W), and the points of those lines are shown in the location map in Figure 11. The electrical resistivity data were acquired and accumulated for the purpose of mapping this site along the two dimensional (2-D) electrical resistivity profiles, in excess of, or beneath the sinkhole, using a 61-channel array in the Wenner design. The measurement length of each profile was 400 m, with an electrode spacing of 5 m, on average, spaced at 25 m intervals between each profile. The total length of all profiles in this site was 2400 m, covering an area of 60000 m^2, and 320 data points were composed for each (61-electrode) in one profile. On average, about 1920 data were collected from a total of six profiles at this site.

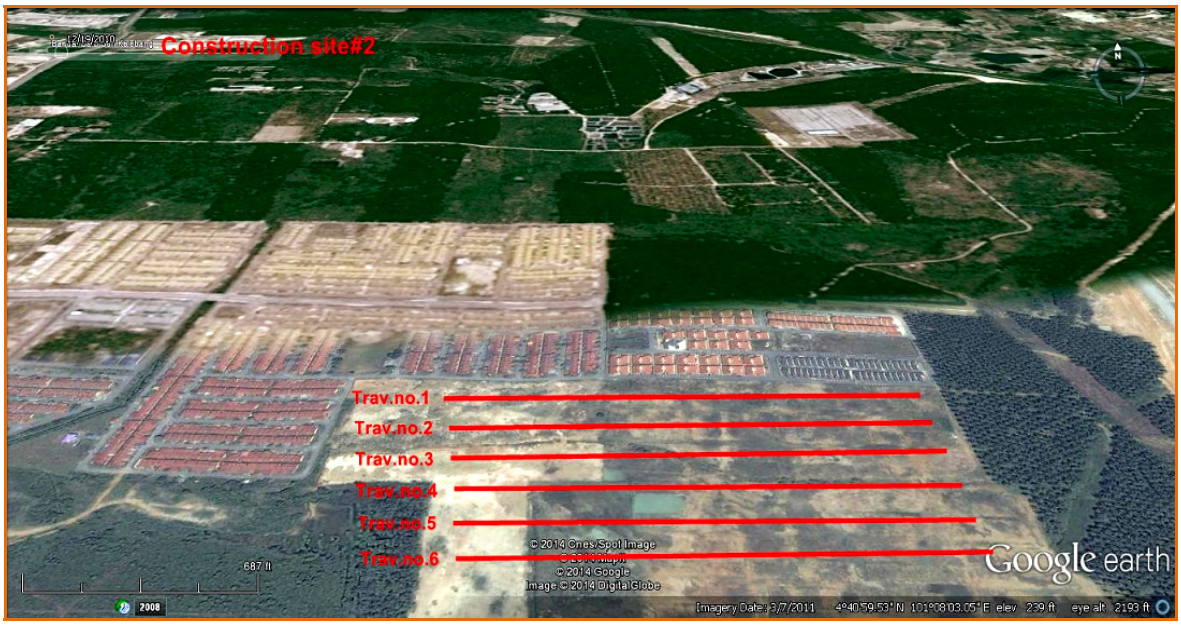

Figure 11. Google earth satellite images (2011) showing the location of resistivity profiles in construction site #2

10. Data Processing

After completing the field survey, the resistance measurements were regularly converted to apparent resistivity values. The data were developed to produce two-dimensional resistivity model of the subsurface. This step is related to convert the apparent resistivity values into a resistivity model section that can be used for geological explanation. The data were readily obtained in the RES2DINV formats, while the conversion program was outfitted with the system. The Root Mean Square (RMS) error statistics enumerated the distribution of the percentage differentiation between the logarithms of the calculated resistivity values, and those calculated from the true resistivity model (calculated apparent resistivity values). Data points containing errors of more than 30% and above are usually omitted. In this survey, a small RMS value is indicative of the fact that less than 10% are defined by the convergence limit. The average default RMS error value in construction site#1 is 6.6%, and the change in the RMS error between iterations was a minimum of 4.0%, and a maximum of 10.5%. The average default RMS error value in construction site#2 is 7.2%, and the change in the RMS error between iterations was a minimum of 4.6%, and a maximum of 9.6%. To get a good model, the data must be of uniformly of good quality.

11. Interpretation of Electric Resistivity Tomography (ERT) Sections

The ERT technique was applied in this geo-electrical survey to investigate the sinkholes, due to its relatively lesser effort and accuracy. It is based on the application of electrical current into the analyzed bedrock, and measuring the intensity of electric resistivity to its conduit. Fundamentally, it provides information of electric resistivity resources via the investigated material towards the electrical current passageway.

Deafening imaging of the bedrocks and features in subsurface karsts terrain is appropriately suitable to render geological classification founded on the variations on electrical resistivity values of the study area into the surface of the soil, clay, weathered rock, intact rock, and air-filled cavities. Clays are usually distinguished by its low apparent resistivities and variables, which are more dependent on moisture, mineral content, purity, and unit

shape/size, usually from 5 ohm-m to less than 60 ohm-m, while sand is usually typified by low apparent resistivity and variables, depending on the moisture content, purity and unit size, usually from 70 ohm-m to less than 160 ohm-m.

Comparatively weathered limestone rock is typified by high apparent resistivity that is typically more than 200 ohm-m to less than 400 ohm-m. Solid or unbroken limestone rock is distinguished by higher apparent resistivity, naturally more than 400 ohm-m to more than 4000 ohm-m, which varies depending on the layers' thickness, its impurities and its moisture content. Air-filled cavities or voids are generally characterized by very high apparent resistivities, classically >3000 ohm-m - 6000 ohm-m, but this varies depending on the conductivity of the nearby strata and the size/shape of void or cavity.

Dolomitic limestone or dolomite with higher apparent resistivity, naturally more than 6000 ohm-m - 80000 ohm-m, varies depending on the layers' thickness. This will form the bulk of the work for electrical investigations survey in these sites for the purpose of understanding resistivity profiles. Hence, electrical resistivity values were resolute for each rock unit. The results are tabulated in Table 3. This table is useful in the context of investigating karst features and its deposits within carbonate karst terrains, while at the same time also being suitable for the purpose of detecting any mineral deposits within the sediments in the area, which requires extensive experience. In the following analysis, key explanatory interpretations were prepared for the geophysical electrical data in the selected study areas.

Table 3. Describes the range of resistivity values with the expected geological unit's deposits

No.	Range of resistivity values	Expected geological units deposits	Color of Res. units in ERT model
1.	0 Ω-m – 5 Ω-m	Insufficient low resistivity, Soft clay with water filled porosity, very high mineralized.	
2.	5 Ω-m – 10 Ω-m	Extremely low resistivity and very high conductivity, soft clay with ponded water, highly mineralized.	
3.	10 Ω-m – 20 Ω-m	Very low resistivity and very high conductivity, Clay moderate mineralized.	
4.	20 Ω-m – 50 Ω-m	Clay low mineralized, low resistivity and very high conductivity.	
5.	50 Ω-m – 70 Ω-m	Below average resistivity, soil, silty or sandy clay.	
6.	70 Ω-m – 100 Ω-m	Average resistivity, clayey or silty sand.	
7.	100 Ω-m – 160 Ω-m	Above average resistivity, sand friable, coarse grain.	
8.	160 Ω-m – 200 Ω-m	Mostly high resistivity, transitional zone consists of rock fragments and sand.	
9.	>200 Ω-m – 400 Ω-m	high resistivity, weathered limestone, probably consisting of wet joints or fractures and/or clay in-fill, higher resistivity	
10.	>400 Ω-m – >3000 Ω-m	Very high resistivity, Compact or intact limestone.	
11.	>3000 Ω-m – 6000 Ω-m	Extremely high resistivity, Voids or cavity, air in-fill.	
12.	>4000 Ω-m – 8000 Ω-m	Extraordinarily high resistivity, Intact pure marbleized limestone or dolostone rocks.	

11.1 Interpretation of Electric Resistivity Tomography Sections in Construction Site #1

The electrical resistivity data of this construction site#1 were building up in electric resistivity tomography sections. The interpretations of tomography or image sections were clarified by applying Table 3 above in the absence of borehole control. The inverse model of electrical resistivity section form travese#1 to traverse#6,

Figure 12 (A-F): viewing the interpreted location of shallow karst features (sinkholes and cavities) in Construction site #1 (Taman Klebang Putra).

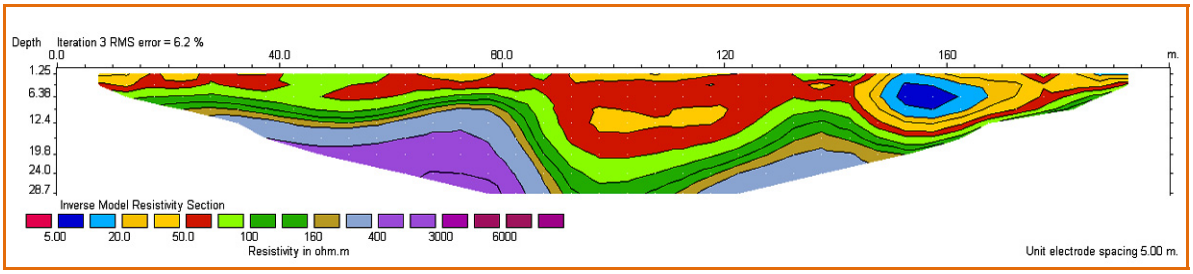

Figure (12-A) Inverse model of electrical resistivity section for profile no. 1 (Taman Klebang Putra)

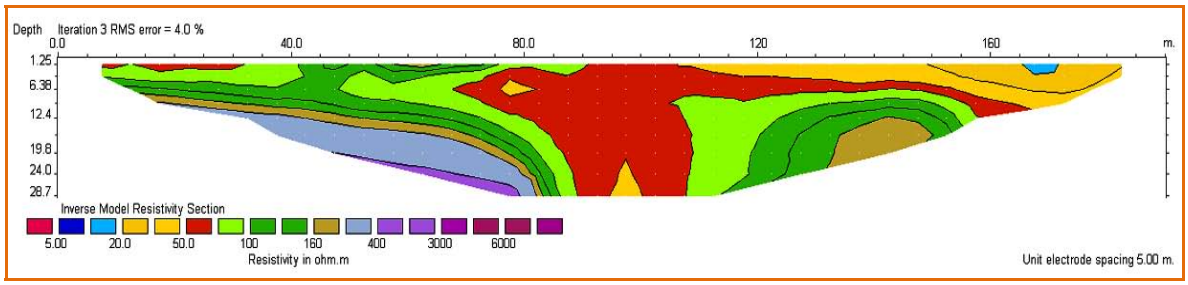

Figure (12-B) Inverse model of electrical resistivity section for profile no. 2 (Taman Klebang Putra)

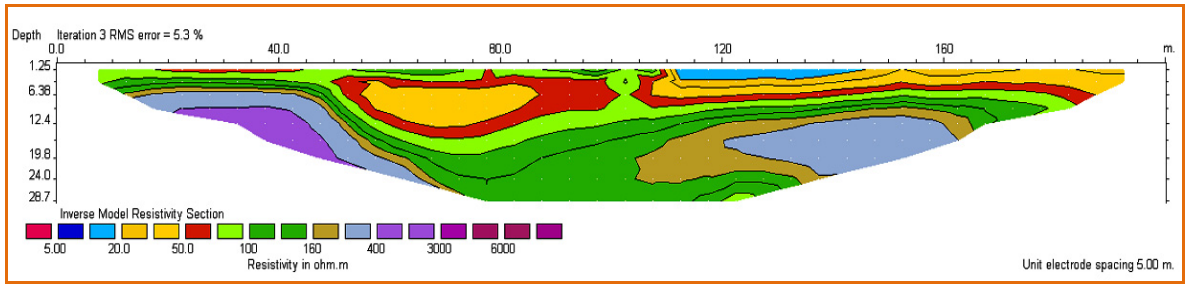

Figure (12-C) Inverse model of electrical resistivity section for profile no. 3 (Taman Klebang Putra)

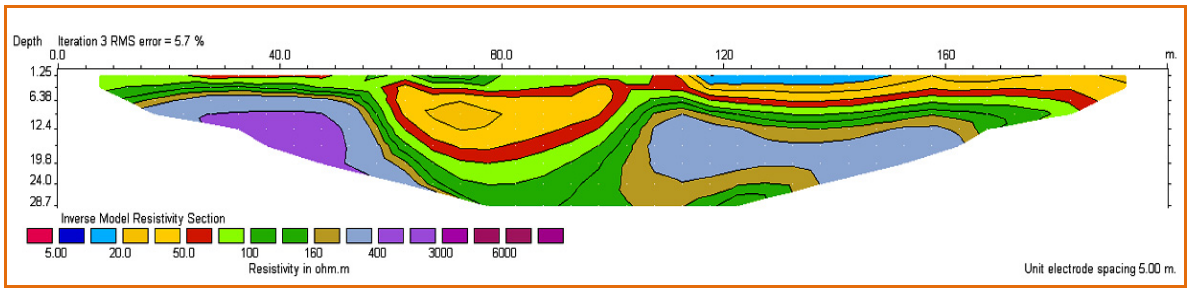

Figure (12-D) Inverse model of electrical resistivity section for profile no. 4 (Taman Klebang Putra)

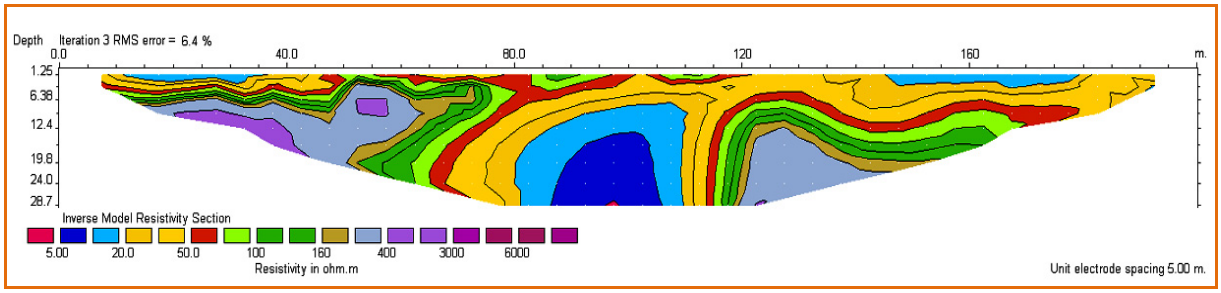

Figure (12-E) Inverse model of electrical resistivity section for profile no. 5 (Taman Klebang Putra)

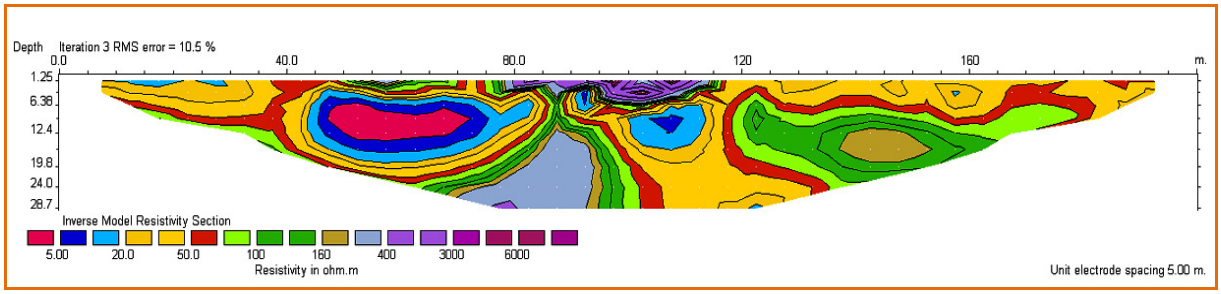

Figure (12-F) Inverse model of electrical resistivity section for profile no. 6 (Taman Klebang Putra)

Figure 12. Inverse model of electrical resistivity section form profiles#1 to profiles#6, viewing the interpreted location of karst features (cavities and sinkholes) in Construction site #1(Taman Klebang Putra)

This site is located in the West flank of Kinta valley, situated over a high topographic area and a flat terrain of marbleized limestone rocks, covered with soil. In resistivity Profile #1, the sinkhole appears in the core between electrode 17 and electrode 28, with an unbalanced center between electrode 21 and 22, Figure (12-A). It stretches in resistivity Profile #2 under these same aspects. In resistivity Profile #4, the position of this sinkhole differentiates, forming itself between electrode 12 and electrode 23, with an uneven center between electrodes 19 and 20 (Figure 12-D). In resistivity Profile #6, the position of this sinkhole varies, and also comes into view between electrode 18 and electrode 26, with an uneven center between electrodes 21 and 22, Figure (12-F). The depth of this sinkhole varies; in resistivity profile #1, it commences from the shallowest subsurface depth of <3.0m, and continues down to a depth of >28.7 m, the bottom being unnoticeable with same aspect mirroring resistivity profiles #2, #3, #4, #5 and #6.

This sinkhole comprises of sediments, with several categories of resistivity values with wide differences, ranging between < 5 Ω-m and 160 Ω-m. In resistivity profiles #1 and #2, the range differs between 20 Ω-m - 160Ω-m, while in resistivity profiles #3 and #4, the range differs between 50 Ω-m - 160Ω-m. Finally, in resistivity profiles #5 and #6 the variation in the range virtually between < 5Ω-m - 160 Ω-m.

The ideal representation of sediments section placed in this sinkhole originated from resistivity profile#5, with resistivity values in the range between 5 Ω-m - 160 Ω-m. The section appears from the upper subsurface downward are as follows:

- Top deposits, low mineralized clay with low resistivity.
- From then on, sandy or silty clay with average resistivity.
- Subsequently, silty sand with average resistivity.
- Afterward, sand with above average resistivity.
- Beneath this, transitional zone consisting of limestone rock fragments and sand with high resistivities.
- In the middle of this sinkhole, several categories of resistivity values appear as follows:
- Soft clay with pond water, highly mineralized, extremely low resistivity's and very high electrical conductivity opening in the middle of sinkholes from a depth of 14.0 m to attain a depth of > 28.0 m.
- Moderate mineralized clay with very low resistivity's and elevated electrical conductivity adjacent the upper irregularity from a depth of 6.38 m, to reach a depth of > 28.0 m.

This suggests that the origin of this sinkhole might be from pre-existing fractures, which probably was widened due to subsidence movement in the area, causing the top layers to crumble down onto the limestone bedrock. This is then swiftly filled with clay and other materials due to the activity of run-off water on its face. In resistivity profile #1, patterns of lower resistivity representing oval – shaped lens are experimental between electrode 30 to electrode 36 in the shallowest subsurface from a depth of < 2.25 m, onwards to a depth of ~ 12.4 m. This lens contains deposits with resistivity's values in the series of 5 Ω-m – 50 Ω-m. Anomaly with patterns of lower resistivity representing depression with tubular – shapes were detected in resistivity profile #3 (Figure 12-C), at the subsurface directly to the right flank between electrode 23 and electrode 30, and from a depth of ~1.25 m, enduring down to a depth of < 6.38 m. This depression bears several types of resistivity values in the range of 10 Ω-m - 70 Ω-m. This abnormality mostly consisted of organic gray clay, which is deposited from the old swamp, partially extended into resistivity profile #2, and visibly into resistivity profile #4 and profile #5. A supplementary anomaly, similar to that described above, was detected in resistivity Profile #5 (Figure 12-E), containing several categories of resistivity values in the range of 10 Ω-m - 70 Ω-m, at the shallowest subsurface directly at the left flank between electrode 3 and electrode 8, commencing from a depth of ~1.25 m, and continuing down to a depth of < 3.0 m.

Table 4. Database of karst features from the inverse model sections in construction site#1

Data base of karst features from (2-D) E. R. Tomography sections in construction site #1 (Taman Klebang Putra)						
TRAVERSE NO.	KARST FEATURES	QUANTITY	LOCATION	SIZE	APPROXIMATE DEPTH	DESCRIPTIONS
Trav.#1	Sinkhole	1	E17-E28	Diameter~55.0m	~1.25m->28.7m	Subsidence sinkhole, in-fill with stiff, non stiff clay, silty and sand.
	Lens	1	E30-E36	Width ~30.0m	>2.25m- ~12.4m	Oval shape lens in-fill with non stiff clay and ponded water.
Trav.#2	Sinkhole	1	E15-E28	Diameter ~65.0m	~1.25m ->28.7m	Subsidence sinkhole in-fill with stiff clay, non stiff, silty and sand.
Trav.#3	Sinkhole	1	E10-E27	Diameter ~85.0m	~1.25m - ~24.0m	Subsidence sinkhole in-fill with stiff clay, non stiff, silty and sand.
	Small Depress	1	E23-E30	Length~35.0m	~1.50m - ~9.0m	In-fill with non stiff and stiff clay.
Trav.#4	Sinkhole	1	E12-E23	Diameter ~55.0m	~1.25m - >24.0m	Subsidence sinkhole in-fill with stiff clay, non stiff, silty and sand.
	Small Depress	1	E24-E31	Length ~35.0m	~1.50m- ~11.0m	In-fill with stiff and non stiff clay with ponded water.
Trav.#5	Sinkhole	1	E16-E26	width ~50.0m	~1.25m - >28.7m	Subsidence sinkhole in-fill with stiff clay, non stiff, silty and sand.
	Small Depress	1	E27-E34	Length ~35.0m	~ 0.0m - ~12.4m	In-fill with stiff and non stiff clay with ponded water.
Trav.#6	Sinkhole	1	E18-E26	Diamerter ~35.0	~1.25m - >28.7m	Subsidence sinkhole in-fill with stiff clay, non stiff, silty and sand.
	Lens	1	E10-E18	width ~ 40.0m	~1.25m - ~23.0m	Oval shape, packed with non stiff clay and ponded water.
	Lens	1	E24-E27	width ~15.0m	~ 4.50m- ~18.0m	Oval shape, packed with non stiff clay and ponded water.
	Cavity	1	E25-E34	width ~ 45.0m	~11.0m - ~15.0m	Packed with rock fragments.
	Depression	1	E26-E35	Length ~ 45.0m	0.0m - ~9.0m	In-fill with stiff clay.

Most of the sediments that are deposited in resistivity profile #6 form oval - shaped lenses, consisting of diverse patterns of resistivity values, one of which was shown in the subsurface directly at the left flank between electrode 10 and electrode 18, from a depth of 1.25 m down to a depth of 23.0 m, also containing several categories of resistivity values in the range of > 5Ω-m - 50Ω-m, and appearing from the core, extending outwards as follows:

Vastly mineralized soft clay with ponded water, extremely low resistivities, representing the core of the lens.

Moderately mineralized clay with very low resistivites adjoining the core.

Low mineralized clay with low resistivities in the external most layers of the lens.

The uppermost of the subsurface layer in resistivity profile #6 were of higher resistivity, representing boulders of weathered limestone, and/or fragments of limestone or other rocks, gravel amalgamated with friable sand, emerging between electrode 11 and 14, then between electrode 17 and 24, from a depth of 1.25 m deep, to a depth of ~ 7.0 m.

A cavity appeared in the sand at the right flank of resistivity profile #6, between electrode 25 and electrode 34, from a depth of ~ 1.0 m to ~15.0 m, typically filled with remaining sediment and rock fragments, Figure (12-F). All Database of the Karst features that are detected through the survey in construction site#1 were described in Table 4.

Figure (12-A, B, C, D, E, F) clearly shows the jointed limestone bedrocks, which are probably made of wet fractured and/or water or clay in-fill, positioned underneath and adjoined to the sinkhole. The surface of this bed was irregular, and contains topography with uplifting and hollow space or pits. This unit indicated the remaining unique limestone formation appearing after a procedure of dissolving into subsurface karsts. The intensity of this bed varies between ~6.5m - ~12.0 m in the left flanks, and tumbling down in the middle of these profiles to get a depth of > 28.8 m, reappearing at the right flank at a depth of ~9.0 - ~19.0 m. Uninterrupted bedrock of undamaged or un-weathered limestone of very high resistivity was found at this site, beneath and adjoining the jointed limestone observed in the left flank at a depth of ~8.0 m - ~15.0 m, continuing to be deep in order to reach a depth of >28.0 m at the core of these profiles. It reappears at the right flank, at a depth of ~24.0 m - ~26.0 m. Quite a few pinnacles were observed in the subsurface of this site between a depth of ~6.0 m - ~19.0 m; Figure (12-A, B, C, D, E, F). The intensity of weathered, un-weathered or intact limestone bedrock and the depth of pinnacles in construction site#1 were viewed in Table 6.

11.2 Interpretation of Electric Resistivity Tomography Sections in Construction Site #2

The electrical resistivity data of this construction site#2 were building up in electric resistivity tomography sections. The interpretations of tomography or image sections were clarified by applying Table 3 above in the absence of borehole control. The inverse model of electrical resistivity section form traverse#1 to traverse#6, Figure 13 (A-F): viewing the interpreted location of shallow karst features (sinkholes and cavities) in Construction site #2 (Taman Klebang Restu)

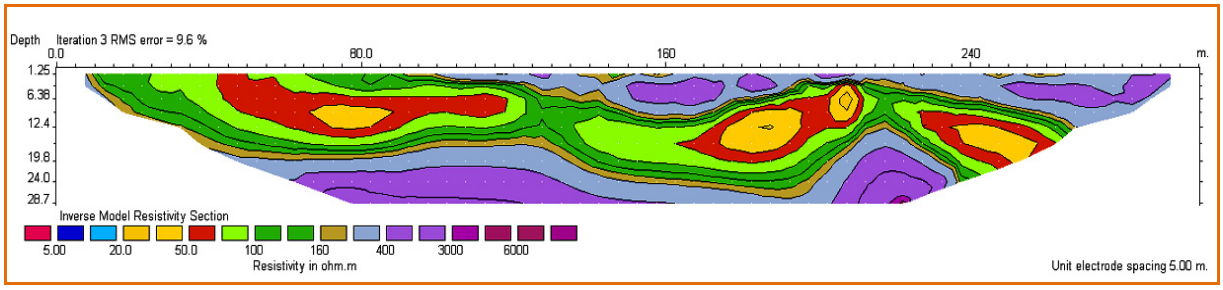

Figure (13-A) Inverse model of electrical resistivity section for profile no. 1 (Taman Klebang Restu)

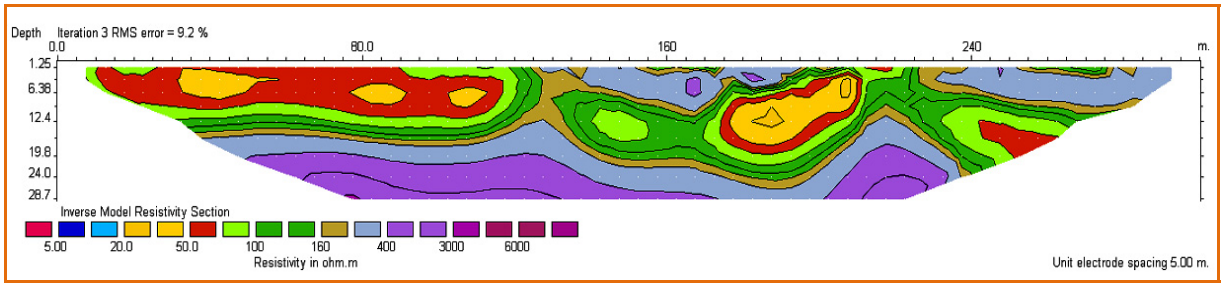

Figure (13-B) Inverse model of electrical resistivity section for profile no. 2 (Taman Klebang Restu)

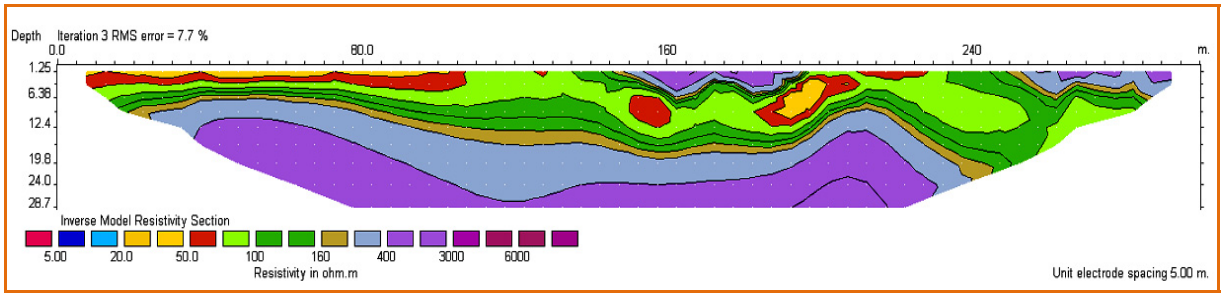

Figure (13-C) Inverse model of electrical resistivity section for profile no. 3 (Taman Klebang Restu)

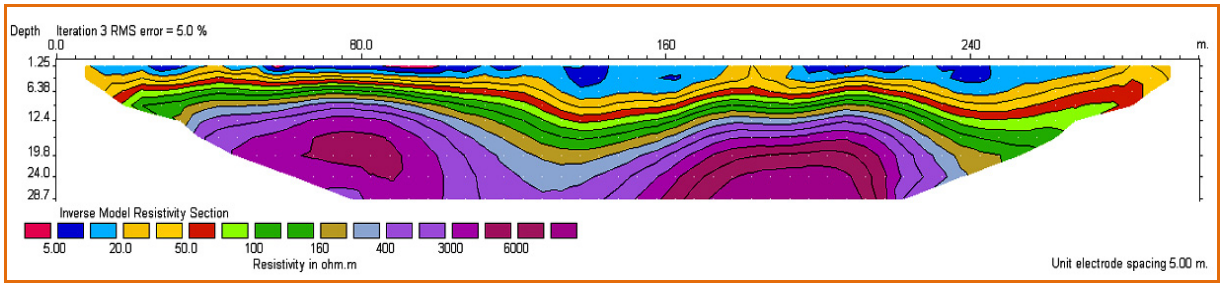

Figure (13-D) Inverse model of electrical resistivity section for profile no. 4 (Taman Klebang Restu)

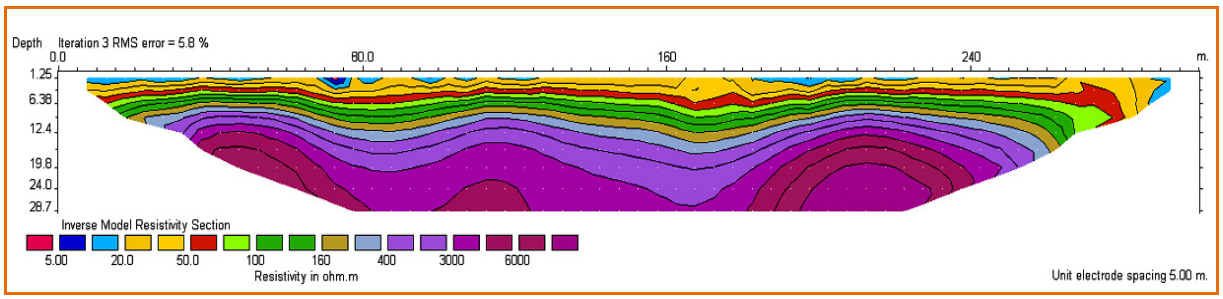

Figure (13-E) Inverse model of electrical resistivity section for profile no. 5 (Taman Klebang Restu)

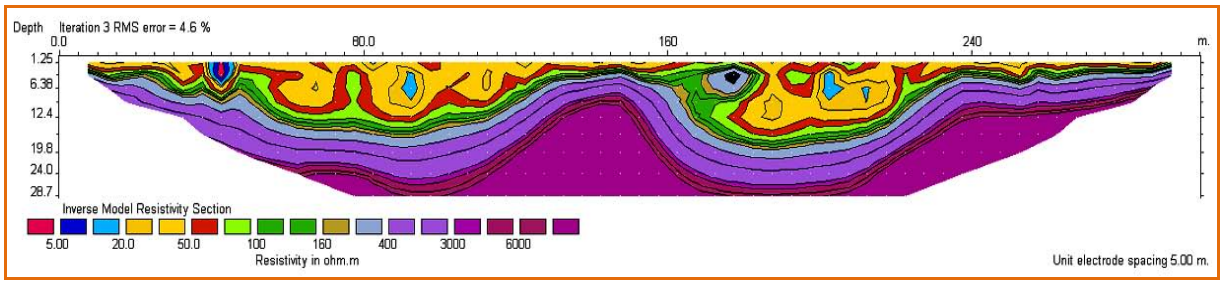

Figure (13-F) Inverse model of electrical resistivity section for profile no. 6 (Taman Klebang Restu)

Figure 13. Inverse model of electrical resistivity section form profiles#1 to profiles#6, viewing the interpreted location of shallow karst features (sinkholes and cavities) in Construction site #2 (Taman Klebang Restu)

The interpretation confirms that a zone of irregular sub-surface magnitudes in this site is extended between resistivity Profile #1and Profile #3 in the shape of one longitudinal asymmetrical tubular channel. Sinkholes were detected near the surface in resistivity profile #2, commencing in the shallowest subsurface between electrode 40 and electrode 58 in the right flank, from a depth of < 1.25 m, sustaining deep in order to reach a depth of ~24.0 m. It appears as a slim to medium wide throat, extending to about 40 m in diameter. The center of the sinkhole appeared in this profile, and was expanded in profile#1 and profile#3. This sinkhole was linked to one or asymmetrical tubular channel along these profiles. Tubular cavities of visually undetermined depth emerged as

oval-shaped lenses, merging together into one tubular channel; Figure 13-(A, B, C).

The abnormality detected in resistivity profile #1, profile#2 and profile #3 commenced approximately from electrode 3 to electrode 55 in profile #1, and to electrode 58 in profile #2, and in profile #3, which originated in the shallowest subsurface from a depth of < 1.25 m, and are sustained deep into the right flank in order to reach a depth of ~24.0 m. It consisted of deposits with several categories of resistivity values in the range of 20 Ω-m to 160 Ω-m, and extends outwards from internal to the external, as follows:

- Low mineralized clay with low resistivity and high conductivity coming out as lenses in this tubular incongruity.
- Sandy or silty clay with below standard resistivity surrounding the deposits before.
- Silty sand with standard resistivity representing the key deposits.
- Sand with above standard resistivity.
- Rock part of limestone and sand with high resistivities.

This implies that the base of all these cavities were from a pre-existing features of joints in the limestone bedrock that was probably created into prominent solution-widened joints. Due to the activity of heavy rain and running water on the face, these were then rapidly packed with clay and other materials.

The region of weathered limestone or highly jointed limestone bedrocks extending across these three profiles was seen to be beneath and closest to this longitudinal tubular irregularity, with an overall rough surface, and categorized with higher resistivities. It occurs on the subsurface at a depth of 6.36 m - ~9.0 m, and moved downwards to reach a depth of ~12.0 m - ~17.0 m at the core of this profile, then dropped down to reach a depth of~17.0 m -26 m. After that, it again rises up to reach a depth of~7.0 m-12.0 m in the right flank; Figure (13-A, B, C).

Undamaged or non-weathered limestone bedrocks with very high resistivity were discovered in the subsurface at a depth of ~19.8 m along the left flank, in profile #1, profile#2 and profile#3. It tumbled down to achieve a depth of >27.0 m in the core, and continued to the right flank, arising up in the shape of a crest in order to reach a depth of ~12.4 m, Figure (13-A, B, C). Numerous pinnacles of limestone were observed in the subsurface in profile #1, profile #2 and profile#3, which were at a depth of ~11.5 m - ~12.4 m, Figure (13-A, B, C). In Resistivity Profile#4 and Profile #5, the cover karst deposits expanded from electrode 3 to electrode 58. Two depressions were observed in the resistivity section, one of which was between electrodes 10-36, while the other between electrodes 40-56. The utmost depth of these depressions was between ~11.5 m - ~13.0 m for the one at the center of this profile, and a depth of ~13.5 m for the one in the right flank of this profile, Figure (13-E).

A number of categories of resistivity values in the range of 20Ω-m to 160 Ω-m emerged with these deposits. Limestone bedrock with karstification features was clearly detected in the subsurface of both flanks, with twin centers appearing beneath electrode 29 and electrode 49 in resistivity Profile#4. It comes with a tri-center in resistivity Profile#5. This irregular zone of weathered limestone expanded across this profile beneath the upper layers, which was overall characterized by higher resistivity; starting in the subsurface at a depth of ~6.36 m, to make a maximum depth of ~15.5 m. Also, in these profiles, intact or unweathered limestone bedrock was found at a depth of ~7.5 m to ~12.0 m in the left flank, plunging down at a depth of ~9.0 m - ~22.0 m in the center, and at a depth of ~17.0 m to - 24.0 m in the right flank. Several pinnacles of limestone were discovered in the subsurface beneath these profiles at a depth between ~6.0 m - ~7.0 m, Figure (13-D, E).

In resistivity profile #6, two depressions were observed in the resistivity section; one between electrode 3 and electrode 29, with a maximum depth of ~15.5m beneath electrode 19, while the other depression was between electrode 30 and electrode 57, with a maximum depth of ~18 m beneath electrode 39. Additionally, deposits with numerous categories of resistivity values are crammed with these depressions, ranging from 20 Ω-m to 160 Ω -m, and lenses of lower resistivity values from 10 Ω-m to 20 Ω -m were found in the middle of these depressions. Moreover, mature cavities were located in the sand, between electrodes 35 and electrode 37 at a depth of ~1.25 m, down to a depth of ~8.0 m, ~10 m wide, and ~6.75 m height, with enormously high resistivity that are typically air-infilled, Figure (13-F).

Immediately before electrode 9 till electrode 10, a small sinkhole was observed from the surface down to a depth of ~8.0 m, containing several categories of resistivity values ranging from 5 Ω-m to 20 Ω-m. This sinkhole water is in-filled, and typically consists of soft clay with ponded water. Sufficiently mineralized clay was found adjacent to the preceding deposit, Figure (13-F). The existence of clay deposits observed in this site could compromise the site's reliability, as the clay could fall down or disrupt piping when situated under load, due to the weight of the

structures. All of the Karst features, which were detected through the survey in construction site #2, were described in Table 5.

The limestone bedrock that was visibly observed in the subsurface along this profile possesses very high resistivities. With the development of karstification phenomena, which describes the rough carbonate bedrock containing many peaks and troughs, starting with a zone of weathered limestone, and/or highly widened jointed limestone bedrock expanding across this profile, overlooking the upper layers at a depth of ~3.5 m down in order to reach a maximum depth of ~18.0 m that was overall characterized by higher resistivity. This was maintained by intact or unweathered limestone bedrock with very high resistivity, observed on the subsurface at a depth of ~4.0 m on both flanks, tumbling down to reach a maximum depth of ~22.0 m in the centre.

Limestone pinnacles were noticeably observed at the subsurface in the middle of this resistivity profile, between depths of ~3.5 m to ~4.0 m Figure (13-F). The depth of weathered, unweathered or integral limestone bedrocks and pinnacles in construction site#2 was presented in Table 7.

Table 5. Database of karst features from the inverse model sections in construction site#2

Data base of karst features from (2-D) E. R. Tomography sections in construction site #2(Taman Klebang Restu)						
TRAVERSE NO.	KARST FEATURES	QUANTITY	LOCATION	SIZE	APPROXIMATE DEPTH	DESCRIPTIONS
Trav.#1	Irregular longitudinal tabular channel	1	E3 - E58	Length ~ 260.0m	~9.25m - ~28.7m	In-fill with stiff clay, silty sand and sand.
Trav.#2	Sinkhole	1	E40 - E58	Diameter ~40.0m	<1.25m - ~24.0m	Rain water dissolution activity.
	Irregular longitudinal tabular channel	1	E3 - E58	Length ~260m	~9.25m - ~28.7m	In-fill with stiff clay, silty sand and sand.
Trav.#3	Sinkhole	1	E40 - E58	Diameter~40.0m	<1.25m - ~24.0m	Rain water dissolution activity.
	Irregular longitudinal tabular channel	1	E3 - E55	Length ~260.0m	~ 9.25m - ~28.7m	In-fill with stiff clay, silty sand and sand.
Trav.#4	Depression	1	E10 - E36	width ~130.0m	0.0m - ~17.0m	Due to Karst processes.
	Depression	1	E40 - E56	width ~130.0m	0.0m - ~17.0m	Due to Karst processes.
Trav.#5	Depression	1	E11- E23	Length ~ 60.0m	0.0m - ~ 9.50m	Due to Karst processes.
	Depression	1	E26 - E43	Length ~160.0m	0.0m - ~11.50m	Due to Karst processes.
Trav.#6	Depression	1	E3 - E29	Length ~120.0m	0.0m - ~15.5m	In-fill with stiff and non-stiff clay.
	Depression	1	E30 - E57	Length ~105.0m	0.0m - ~18.0m	In-fill with stiff and non-stiff clay.
	mature cavity	1	E35 - E37	Size ~ 60.75m2	~1.25m - ~8.0m	Air in-fill.
	Small sinkhole	1	E9-E10	Diameter ~5.0m	0.0m - ~ 8.0 m	In-fill with water and non -stiff clay.

12. Depth of Marbleized Limestone Bed Rock in the Study Construction Sites

The Nearby karst terrains normally create problems for civil engineers. Often, only engineers who are familiar with soluble rock understand these anomalies and problems that are associated with it. For engineers, limestone creates various difficulties that are made complex by increased expansion of the karsts morphology. The table below presents an outline or portrayal of some selected points regarding the limestone bedrock depth of the five

construction sites that will be favorable for engineers for them to recognize the depth of limestone in the sites under study. These are, however, incomplete, and can only provide common suggestions of projected ground conditions, despite the possibility of ending up with enormous discrepancies regarding the depth of the local feature.

Table 6. Described the approximate depth of weathered, intact marbleized limestone bedrocks and pinnacles in construction site#1

No.	Site #1(Taman klebang putra)	Electrode No	Approximate depth of weathered marbelized lst.	Electrode No.	Approximate depth of Intact marbleized Lst. bedrock	Electrode No.	Approximate depth of pinnacles
1	Res Trav. #1	7 11 16 18 19 - 24 28	11.0 m 13.0 m 8.0 m 19.8 m >28.0 m 19.0m	8 11 15	15.0 m 18.0 m 14.0 m	16 28	7.0 m 19.0 m
2	Res Trav. #2	5 9 17 18	10.0 m 12.4 m 24.0 m > 28.0 m	10 16 17	19.0 m 24.0 m > 28.0 m	–	–
3	Res Trav. #3	4 12 16 - 25 31	6.5 m 18.0 m > 28.0 m 9.0m	4 9 14	10.0 m 8.5 m > 28.0 m	–	–
4	Res Trav. #4	4 9 13 15 23 33	8.5 m 6.38 m 18.0 m > 28.0 m 9.0 m 12.0m	6 10 12	8.0m 8.0 m 19.8 m	–	–
5	Res Trav. #5	4 10 12 15 26 30	7.0 m 10.0 m 3.0 m > 24.0 m 12.0 m 22.0 m	5 9 10 15 24 26	8.0 m 10.0 m 18.0 m > 28.0 m > 28.0 m > 26.0 m	12 26	3.0 m 11.0 m
6	Res Trav. #6	15 19 20	26.0m 12.0 m > 28.0 m	–	–	–	–

The surveys showed that the depth of marbleized limestone bedrock in these construction sites was uneven or

asymmetrical and possesses many pinnacles and cutters. Table 10 described the approximate depth of weathered, intact marbleized limestone bedrock and pinnacles in construction sites. In construction site #1, the depth of weathered limestone bedrock was mixed between 3.0 m and >28.0 m. For intact limestone bedrock, the depth varied between 8.0 m and >28.0 m, and the depth of pinnacles varied between 3.0 m and 19.0 m, as shown in Table 6. In construction site #2, the depth of weathered limestone bedrock mottled between 1.25 m and 26.0 m. The depth of an intact limestone bedrock varied between 4.0 m and >28.0 m, while the depth of its pinnacles varied between 3.5 m and 12.4 m, as shown in the Table 7.

Table 7. Described the approximate depth of weathered, intact marbleized limestone bedrocks and pinnacles in construction site#2

No.	site #2(Taman Klebang Restu)	Electrode No	Approximate depth of weathered marblelized Lst. bedrock	Electrode No	Approximate depth of intact marbleized Lst. bedrock	Electrode No	Approximate depth of pinnacles
1	Res Trav. #1	21 - 59 9-26 38 44	1.25 m 15.0 m 26.0 m 11.0 m	13 36 44	23.0 m > 28. 0 m 15.0 m	43	12.4 m
2	Res Trav. #2	27 - 40 47 - 57 9-26 26 38 43	1.25 - 16.0 m 1.25 - 9.0 m 15.0 m 12.0 m 26.0 m 12.0 m	11-21 38 44	19.8 m > 28.0 m 17.0 m	26 44	12.4 m 11.5 m
3	Res Trav. #3	6 12 33 43	9.0 m 6.38 m 17.0 m 7.0 m	8 25 43	19.8 m >27.0 m 12.4 m	11 43	6.36 m 9.5 m
4	Res Trav. #4	6 28 43	9.0 m 15.5 m 6.36 m	8 28 43 50	12.0 m 22.0 m 10.0 m 24.0 m	17 43	6.0 m 7.0 m
5	Res Trav. #5	4 17 33 44 54	8.0 m 10.0 m 10.0 m 6.0 m 14.0m	10 24 43 54	7.5 m 9.0 m 8.5 m 17.0 m	10 24 44	6.0 m 6.36 m 6.0 m
6	Res Trav. #6	3 19 30 39 43 59	3.5 m 18.0 m 3.5 m 18.0 m 3.5 m 3.0 m	3 22 30 39	4.0 m 18.0 m 4.0 m 22.0 m	30 49	3.5 m 4.0 m

13. Engineering Classification of Karst Ground Condition

Waltham and Fookes (2003) presented an engineering classification of karstic ground conditions which characterized the simplified guidelines to the potential variation in landforms and ground cavities that may come upon in civil engineering works on karst terrains. This classification divides the Karst terrains into five classes. The five classes confer the basis of an engineering classification that characterizes karst in terms of the difficulty and complexity and to be encountered by the foundation engineer. The geomorphologic characteristics of the five classes are summarized as follows:

• K I: Only in deserts and periglacial zones, or on impure carbonates, sinkholes are rare, rockhead almost uni-form; minor fissures; low secondary permeability, Caves are rare and small; some isolated relict features.

• K II: Minimum in temperate regions, small suffusion or dropout sinkholes; open stream sinks, many small fissures, Fissures are widespread in the few meters nearest surface, Caves are many and small (size less than 3 m across).

• K III: Common in temperate regions; minimum in the wet tropics, many suffusion and dropout sink-holes; large dissolution sinkholes; small collapse and buried sinkholes extensive fissuring; relief less than 5 m , loose blocks in cover soil, extensive secondary opening of most fissures, caves are many (size less than 5 m across at multiple levels).

• KIV: Localized in temperate regions and normal in tropical regions, with many large dissolution sinkholes; numerous subsidence sinkholes; scattered collapse and buried sinkholes, Pinnacles relief of 5-20 m, loose pillars, extensive large dissolution openings, on and away from major fissures, caves are with several size greater than 5 m across at multiple levels.

• KV: Only in wet tropics, very large sinkholes of all types, soil compaction in buried sinkholes, tall pinnacles, relief of greater than 20 m, remnant arches, loose pillars undercut between deep soil fissures abundant and very complex dissolution cavities, numerous complex 3-D cave systems cave size greater than 15 m across, with chambers and galleries).

14. Results and Discussion

The current Electrical Resistivity Tomography (ERT) survey at two housing complex construction sites in the north of Ipoh was conducted in order to determine the subsurface geological features, including sinkholes, karstic voids or cavities, together with the subsurface geological structures such as intensely fractured zones and faults. An assessment of the situation was summarized from the subsurface images. Subsequently, an estimation of the possibility of a collapse occurring due to these sinkholes was prepared.

This study also displayed that high resolution Electrical Resistivity Tomography (ERT) can be effectively employed to reflect the bedrocks and the fractures in subsurface karstified carbonate region. The resistivity method used in this study was very favorable towards locating the underground sinkholes, voids or cavities and also water channels and pipes due to the dissolution processes in fractured zones. It is also completely suitable for differentiating surficial soil, clay, weathered rocks, compact or intact rocks, and air-filled karstic voids or cavities, and intensely fractured rocks. These features effect many construction sites located in areas extended over carbonate rocks, causing disturbance in construction works, which can increase the overall cost of the projects.

The geological model is clarified via the geophysical data, consisting of a basal limestone unit, which comprises of the bedrock; enclosed by soil or sandy clay. This bedrock unit appears to have been dissected or intervened by cavities that are high-flying to solution-widened joints, and is perceived as the karstic processes. These features are perilous, because they are in-filled with thick clay, while others with sandy or salty clay, which could collapse when subjected to piping under load.

The geophysical data indicated that the depth of limestone bedrock was asymmetrical or uneven, containing many pinnacles and cutters. In construction site #1, the depth of weathered limestone bedrock was mixed between 3.0 m and >28.0 m. For intact limestone bedrock, the depth varied between 8.0 m and >28.0 m, and the depth of pinnacles varied between 3.0 m and 19.0 m, as shown in Table 6. In construction site #2, the depth of weathered limestone bedrock mottled between 1.25 m and 26.0 m. The depth of an intact limestone bedrock varied between 4.0 m and >28.0 m, while the depth of its pinnacles varied between 3.5 m and 12.4 m, as shown in the Table 7.

The geophysical data in construction site #1 is indicative of an area of lower resistivity and high conductive anomaly, where the top layers had been lowered by fractures along the site and the resulting sinkhole due to the collapse, thus containing soft clay with vast mineralization with some pond water has made the area less resistive to electrical currents. This was noticed on the site during excavation works. The data also exposed that this sinkhole continues to be produced in the subsurface mostly at this site, and was in fact extended in six locations of the six resistivity profiles at this site.

The geophysical data in construction site #2 showed an area of lower resistivity and high conductive anomaly, which has been affected by longitudinal tubular channel containing clay and sandy clay. The bedrock unit appears to be attacked by many features such as sinkholes, cavities and channels. These features are harmful as they are packed with thick clay, sandy or silty clay, which could collapse when subjected to piping under load. The high resistivity anomalies are indicative of the existence of karstic voids, which require confirmation via drilling results.

These analyses led to the conclusion that the origin of the sinkhole and cavities in construction site#1 was a pre-existing fracture that had widened, possibly due to subsiding movement in the area, causing the collapse of top layers down onto limestone bedrock, which was then rapidly crammed with clay due to the activity of run-off water on the surface. However, the origin of the irregular tabular channels, sinkholes and cavities in construction site#2 appears to be newly developed than the one in site#1. The origins of all these features were previously thought to be of pre-existing features, such as joints in limestone bedrock. It had formed into a strongly outstanding solution-widened joint for rainfall activity and running off rain water on the surface, which was swiftly packed with clay and other materials.

The sinkholes in the study area were characterized by referring to the mechanisms of the ground malfunction, and the nature of the material, which fails and subsides. In construction site#1, the sinkhole is a collapse, which is a type created by a small-scale collapse that provided the surface with subsurface structural features. Then, the earliest collapse sinkhole was packed with soil, sediment and fragments due to the modifications to the surroundings, and finally resulting in the sinkhole being buried. Surface subsidence may then take place, due to compaction of the soil.

The sinkhole in construction site#2 is a type of suspension sinkhole, created by the slow dissolution of the limestone bedrock. They are common features, such as joints of a karst terrain developing over geological time scales. The larger features still have potentially unsound rock mass somewhere beneath their lowest point, and the majority dissolution features are deep holes and pipes. These are produced at isolated stream sinks and swallow holes, where the form resembles conical sinkholes, largely created by scattered water percolation.

The geophysical data also indicated that sinkholes originated from many locations. The most hazardous area was found to be underneath resistivity profile#6 in construction site#1, with sinkholes extending over 55 m and reaching depths of more than 28.7 m. Another harmful area was beneath resistivity profile#6 in construction site#2, with two main depressions. One of them extending 75.0 m with a maximum depth of ~15.5 m, while the other extending about 55.0 m with maximum depth of ~18.0 m. These features are harmful because some are in-filled with thick clay, while others are in-filled with sandy or silty clay that could collapse when situated under a load, due to the weight of the structures.

In accordance to the characteristics of the morphological features of karstic ground conditions by Waltham and Fookes (2005), the karst level in construction site#1 found between profile 1 and profile 6 is a complex karst type KIV, while the karst level in construction site#2 found between profile 1 and profile 3 is a mature karst type KIII. Afterwards, the karst type changed over profile#4 to profile #6 to a complex karst type KIV

Once the excavating work over the resistivity profile#5 was started in construction site#1, the underground water flows up straightforward; which confirms that the geophysical survey there was a body of ground water source under this profile.

15. Planning to Minimize the Risk in Construction Sites Developing over Karstic Carbonate Bedrock by Applying of Engineering Subsurface Remediation Techniques

The variety of foundation which is well-designed for these construction sites over carbonate karst section depends upon the expect foundation loading and the degree of maturity of the karst features. The most dangerous site was this occupied to foundations over sinkholes which was affected by two controlling factors, the overloading expect and the water seeping through the cover soil.

If the problem level of construction site over carbonate karst region are known and classified, the most economical point of view in developing this site is to minimize the risk of structures that are founded over the area by determining the safest direction in changing the plan's location. If possible, the most important part with a great size and type of construction structures has to be placed in the safest region, while the problem areas can be allocated for non-critical facilities, such as grass field, parking lots, golf courses, roadways etc. Controlling the surface and subsurface water drainages must be put in the plans when the work is commencing at these respective sites.

15.1 Three Solutions Were Most Generally Used in the Plan in Order to Minimize the Risk of the Problem Areas in Construction Site#1 (Klebang Putra)

The first solution:

Sinkhole remediation was achieved by utilizing the reverse graded filter technique. To fill this huge sinkhole, the hole must be excavated, and its throat plugged by concrete block, sealed with a thick grout of cement, or fill the hole with larger boulders or rocks at the bottom, followed with a cobble, then gravel or bentonite mixed with rock fragments, then sand, and finally, the top must be covered with 8-12 inches of bentonite and soil. The placement of

larger materials directly on the bedrock at the bottom of the sinkhole is done in order to provide support and prevent another collapse, while the smaller materials stops water from moving the soil downward into the void, and into the bedrock. Sinkhole remediation by utilizing the reverse graded filter technique viewing as shown in Figure 14.

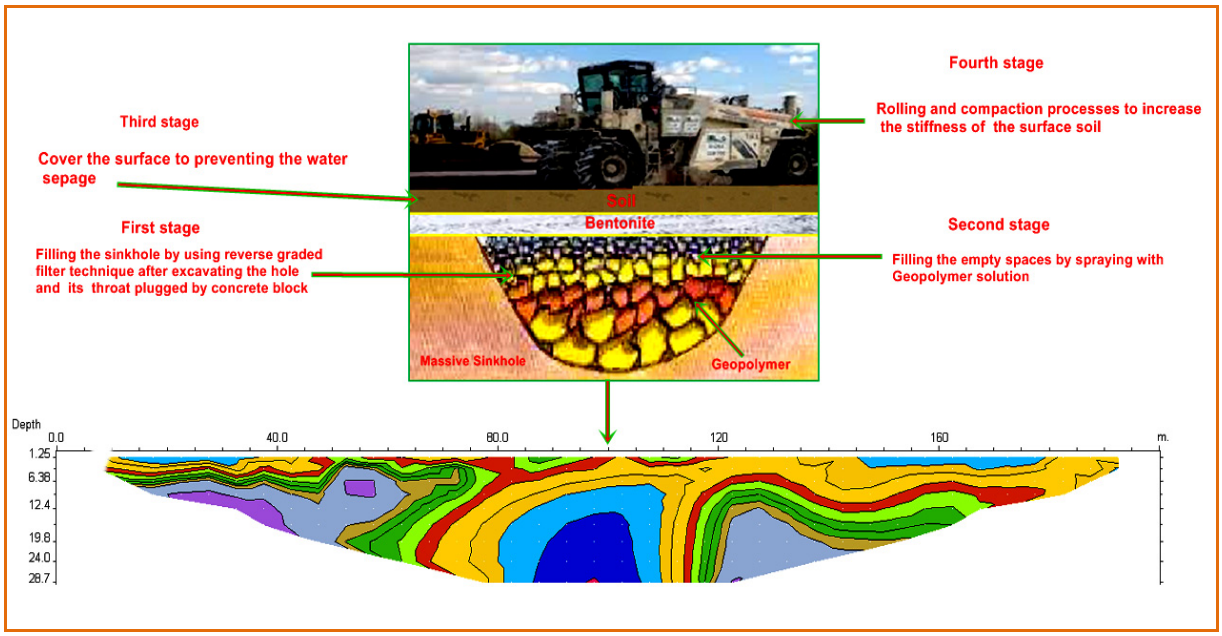

Figure 14. Viewing Sinkhole remediation by utilizing the reverse graded filter technique

The second solution:

The Sinkhole remediation employs the concrete bridge beam in order to transfer the load of constructions to both sides of the massive sinkhole. The application of this method consists of four main stages. The first stage, driven long bearing pier or column down to a point where rest is to the sound rock strata. This column or pier will transfer the loaded weight of the bridge to the ground. The second stage, setting of a concrete support block which provides the support to the two end parts of the bridge. The third stage, filling the hole with larger boulders or rocks at the bottom, followed with a cobble, then gravel. If the sinkhole is very dangerous to the designed foundations, it must be packed with concrete. Sinkhole remediation employs concrete bridge beam as shown in Figure 15.

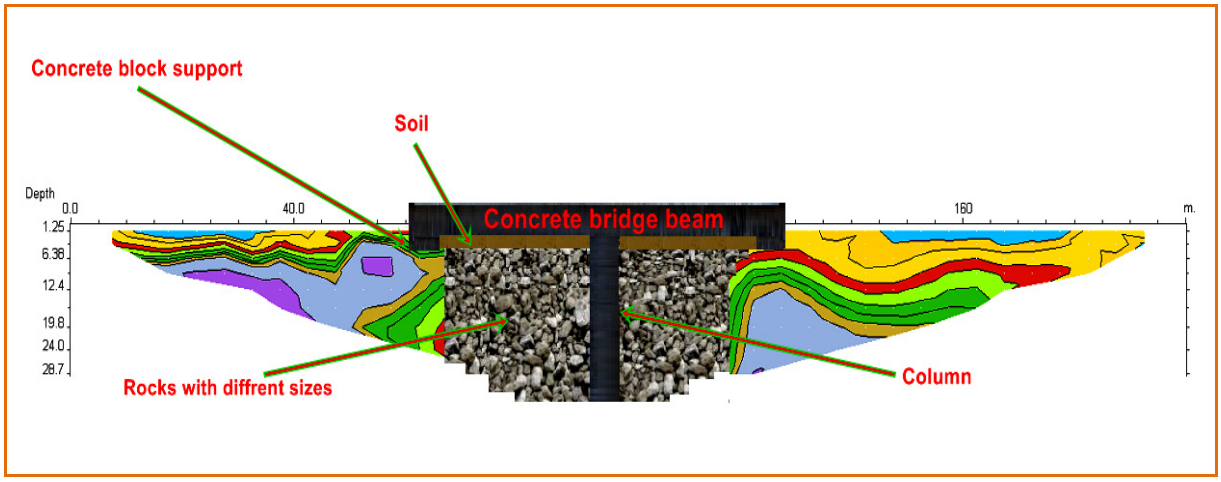

Figure 15. Sinkhole remediation by employing concrete bridge beam in order to transfer the load of constructions to the both sides of the massive sinkhole

The third solution:

If it's possible, relocation is the most important part with a great size and type of construction structures to be placed in the safest region, which may prove to be more cost-effective in certain cases. While the problem areas can be allocated for non-critical facilities, such as grass field and parking lots.

15.2 Four Solution Methods Are Frequently Used in the Plan to Diminish or Minimize the Risk of the Problem Areas in Construction Site# 2 (Klebang Restu)

The first solution:

filling the channels by using chemical grouting process with geopolymer solution forms, can be utilize to fill the fractures, small voids and the cavities in the subsurface layers. Chemical grouting is well suited for channels, and for stabilizing the soil around the channel for mitigating the settlement of overlying structures within the influence of the channel's configuration. Grout is injected into drilled holes along the flow paths of the channel, sealing and preventing the flow of any rainwater through them in the future. The deep chemical grouting by injection of geopolymer solution form is one of engineering subsurface remediation technique presented in Figure 16.

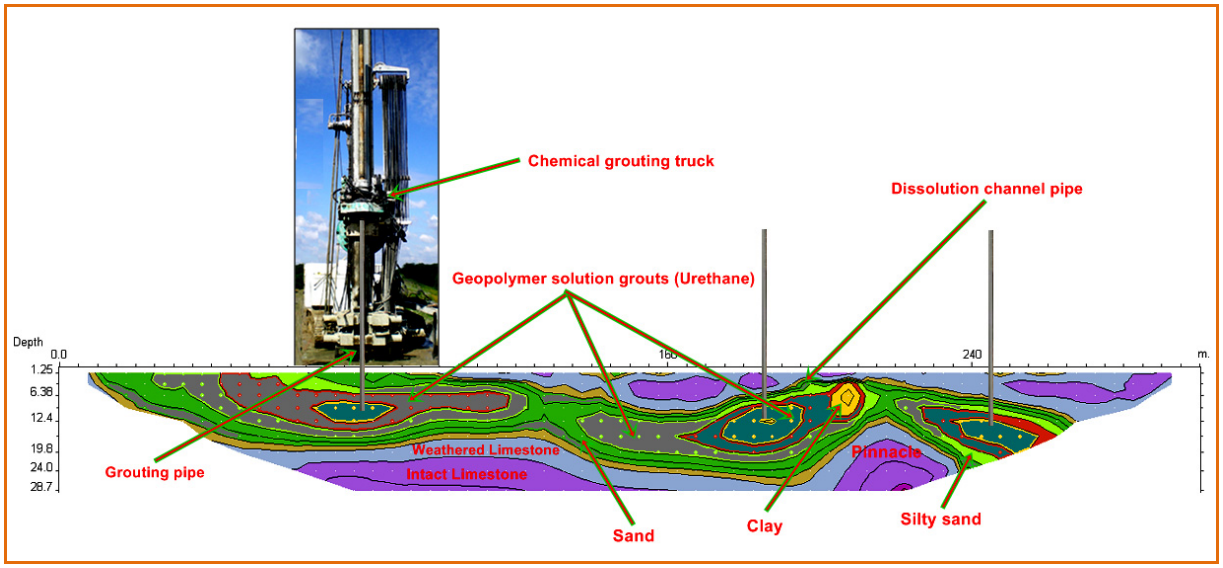

Figure 16. present the deep chemical grouting by injection of geopolymer solution form which is one of engineering subsurface remediation technique in construction site#2

The second solution:

Soil improvement through improving the ground surface by compaction process to increase the stiffness and behavior capacity of the soils through decreasing the permeability.

The third solution:

Place shallow spread footings at regular intervals to transfer the load from the building down to the footings. In this location, a relatively stiff layer (bed rock) exists with shallow depth about 3.0m. In this case, it is usually more economical to use concrete footings as foundation support for the building. The footing effectively spreads the weight from the building column over an area, so that the contact pressure is lower than what the ground can support. Typical spread footings under construction in construction site#2 was presented in Figure 17.

The fourth solution:

Skin friction piles can be driven down through the softer material to specified depth in this construction site. In this type of pile, the load bearing resistance derived on pile mainly from skin /friction resistance along the side of the pile shaft, so that the friction of the soil against the sides of the pile is enough to resist any downward movement.

The high capacity of friction piles has developed a considerable load carrying which is a function of vertical support from skin friction developed between the surface of buried pile shaft area and the contact with the surrounding soil. The Skin Friction Piles that is driven into softer soil (silty, clay and sandy soils) without come across as a stiff or intact layer (bedrock) in construction site #2 presented in Figure 17.

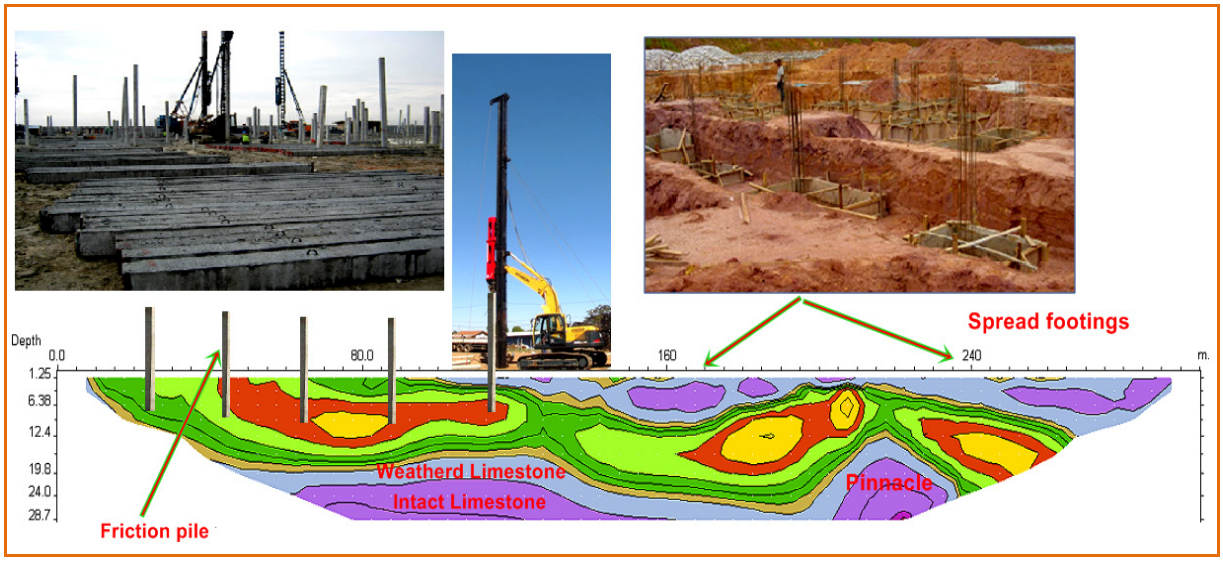

Figure 17. Presenting the Skin Friction Piles and spread footings under construction in construction site #2

16. Suggestions for Future Survey in Kinta Valley

This case study describes the application of Electrical Resistivity Tomography (ERT) technique and aerial photography over two sites of housing complex construction projects, which are situated over a covered carbonate karst region. The hazards of the sinkholes and other karst features such as, cavities and dissolution channel pipe can cause problems to the construction projects in the near future resulting from mismanagement during the initial phase of the projects, as the developers did not carry out prior geophysical technique and geological studies. Moreover, the borings within these karsts regions is incapable of providing sufficient subsurface data for analysis. This might misrepresent the subsurface geological model, which might in turn lead to additional cost for corrective design or ad-hoc analysis. The results of applying the techniques were discussed and the suggestions are:

I. The respective states must implement and enforce a regulation that no construction project may begin in an area over carbonate karst until the geological and geophysical survey is completed in order to avoid any future catastrophic problems.

II. The best plan in future survey is by applying (ERT) technique using a space interval not more than 10m between two parallel lines, because of high lateral variation in the subsurface topography and lithology. Besides to give clear image to the subsurface.

III. Future survey by applying Electrical Resistivity Tomography (ERT) technique which must be developed using 3D ERT survey technique and 3D software to provide a clear image for the subsurface features and structures, and also to provide clear indications of their directions and extent under the subsurface.

IV. Using the borings method to support the result of the (ERT) techniques survey to position which needs early plans to minimize the hazard of sinkhole and other karst features in any construction sites over covered karstificated carbonate bedrock before the start of the construction project.

17. Conclusions

This case study focusing on the application of Electrical Resistivity Tomography (ERT) and aerial photographs to identify consequences of sinkhole hazards in construction housing complexes sites over karstic carbonate bedrock in north of Ipoh, Perak, Peninsular Malaysia.

The techniques were performed across two construction sites. Construction site #1 is located in Klebang Raya and construction site #2 is located in Klebang Restu, Perak. The ERT technique was used in this geoelectrical survey in order to image the subsurface and investigate the karst features such as sinkholes, cavities, depressions and channel pipes, due to the fact that this technique is suitable for differentiating surficial soil, clay, sand, weathered marbleized limestone bed rocks, intact marbleized limestone bed rocks, water - air-filled cavities, and channel pipes. Also, the simplicity of its application was also a major factor in its application decision and due to its less

relative effort and time effectiveness.

The interpretation of E R Tomography/ image sections revealed that many anomalies with very low resistivity and high conductivity extend along the project areas in these construction sites. Massive sinkhole has affected many sections of the project area in construction site #1. Enormous longitudinal channel pipe has affected many sections of project area in construction site #2. An assessment of the situation was surmised from the subsurface images. Subsequently, an estimation of the possibility of a collapse occurring in the near future due to the sinkhole was prepared.

Also, the image sections specified that the depth of the limestone bedrock was asymmetrical or uneven, containing many pinnacles and cutters. Within these karsts areas the boring method is incapable to provide sufficient subsurface data for analysis and may misrepresent the subsurface. In the closing stages one cannot give a clear picture or model to the subsurface, which may lead to additional costs for corrective design or additional analysis.

The karst level in construction site site#1 found between profile 1 and profile 6 is a complex karst type KIV, while the karst level in construction site#2 found between profile 1 and profile 3 is a mature karst type KIII. Afterwards, the karst type changed over profile#4 to profile #6 to a complex karst type KIV.

The hazards of the sinkholes and other karst features such as, cavities and dissolution channel pipe can cause problems to the construction projects in the near future resulting from mismanagement during the initial phase of the projects, as the developers did not carry out prior geophysical technique and geological studies. Moreover, the borings within these karsts regions is incapable of providing sufficient subsurface data for analysis, and this might misrepresent the subsurface geological model, which might in turn lead to additional cost for corrective design or ad-hoc analysis.

Consequently, early engineering subsurface remediation techniques are needed to minimize the potential of geohazard of sinkholes and other karst features in these construction sites over karstic carbonate bedrock. Initial consideration was to utilize the reverse graded filter technique to fill the massive sinkhole in construction site#1. Skin friction piles were driven into the layers which contain non-stiff materials (soil, clay, silt, sand). Utilizing new chemical grouting technique such as deep injection chemical grouting technique in construction site#2. Controlling of the surface and ground water drainages when work begins at these construction sites. The respective states must implement and enforce a regulation that no construction project may begin in an area over karstificated carbonate bead rock until the geological and geophysical survey is completed in order to avoid any future catastrophic problems.

References

Abdel Qadir, S. O., & Yassin, R. R. (1996). Applications of geophysical techniques on investigation of karst features and its deposits east of Rutbah town / Iraqi Western Desert. Geosurv. / Baghdad – Iraq.

Anderson, N. L., Derek, B. A., & Ismail, B. A. (2007). Assessment of Karst Activity at Highway Construction Sites Using the Electrical Resistivity Method, Missouri, USA.

Beck, B. F., & Herring, J. G. (2001). *Geotechnical and Environmental Applications of Karst Geology and Hydrology* (pp. 341-346). Balkema Publishers.

Chan, S. F. (1986). Foundation problems in limestone area, of peninsular Malaysia. Geotech. Engineering Div., IEM, Sep1986, p. 98.

Chang, K. S., & Wong, S. L. (2009). *The limestone hills and caves of the Kinta Valley* (p. 151). Malaysian Nature Society, Kuala Lumpur, Malaysia.

Chow, W. S., Jamaludin, O., & Loganathan, P. (1996). Geotechnical problems in limestone terrain with emphasis on cavities and sinkholes. *Journal of geological society Malaysia, Dec.1996*, 102-117.

Cobbing, E. J., Pitfeld, P. E. J., Derbyshire, D. P. F., & Mallick, D. I. J. (1992). The granites of Southeast Asian tin belt, Overseas Memoir 10, British Geological Survey of London, pp. 78-86.

Dahlin, T. (1996). 2-D resistivity surveying for environmental and engineering applications. *First Break, 14*(7), 275-283.

David, P., Panagiotis, T., & Konstantinos, A. (2008). Electrical resistivity tomography mapping of beach rocks, application to the island of Thassos (N. Greece). *Environ. Earth Sci., 59*, 233-240. http://dx.doi.org/10.1007/s12665-009-0021-9

Fatihah, R. M., AL-Kouri, O., & Yassin, R. R. (2010). Geophysical And Geospatial Database Of Sinkhole

Occurrences Distribution After Earthquake Tsunami. Southeast Asia international geological conference, Indonesia.

Fischer, J. A., & Candace, R. (1989). Foundation Engineering Construction in Karst Terrain, In Foundation Engineering. Current Principles and Practices, Proc. Conf., Eveston, Illinois, ASCE, USA, 1989, pp. 29-42.

Fontaine, H., & Ibrahim, B. A. (1995). Biostratigraphy of the Kinta Valley, Perak. *Geol. Soc. Malaysian Bulletin, 38*, 159-172.

Gobbett, D. J. (1964). The Lower Paleozoic Rocks of Kuala Lumpur. *Malaysia Federation Museum's Journal, 9*, 67-79.

Griffiths, D. H., & Barker, R. D. (1993). Two-dimensional resistivity imaging and modeling in areas of complex geology. *Journal of Applied Geophysics, 29*, 211-226. http://dx.doi.org/10.1016/0926-9851(93)90005-J

Hoover, R. A., & Saunders, W. R. (2000). Evolving Geophysical Standards. The First International Conference on the Application of Geophysical Methodologies & NDT to Transportation Facilities and Infrastructure Conference Proceedings, Missouri Department of Transportation.

Hu, R. L., Yeung, M. R., Lee, C. F., Wang, S. S., & Xiang, J. X. (2001). Regional risk assessment of karst collapse in Tangshan, China. *Environmental Geology, 40*, 1377-1389. http://dx.doi.org/10.1007/s002540100319

Hussein, I. E., Kraemer, G., & Myers, R. (2000). Geophysical characterization of a proposed street extension in Cape Girardeau, Missouri, Proceedings of the First International Conference on the Application of Geophysical Methodologies & NDT to Transportation Facilities and Infrastructure.

Hutchinson, C. S. (2007). *Geological Evolution of Southeast Asia* (2nd Ed., p. 433). Geological Society of Malaysia (Publ).

Hyatt, J. A., & Jacobs, P. M. (1996). Distribution and morphology of sinkholes triggered by flooding following tropical storm Alberto at Albany, Georgia. *USA Geomorphology, 17*, 305-316. http://dx.doi.org/10.1016/0169-555X(96)00014-1

Ingham, F.T., & Bradford, E. P. (1960). The geology and mineral resources of the Kinta Valley, Perak. Geological Survey District Memoir 9, Federation of Malaya Geological Survey, Ipoh, p. 347.

Ioannis, F. L., Filippos, I. L., & Melanie, B. (2002). Accurate Subsurface Characterization For Highway Applications Using Resistivity Inversion Methods. Geophysics & Geothermic Division, Geology Department, University of Athens, Panepistimiopolis, Ilissia, Athens.

Jammal, S. E. (1986). The winter park sinkhole and central Florida sinkhole type subsidence. *International Association of Hydrological Science Publication, 15*1, 585-594.

Kachentra, N., & Tanad, S. (2007). Application of resistivity survey to investigate sinkhole and karst features in southern Thailand, Geothai'2007, Bangkok, Thailand.

Kochanov, W. (1999). Sinkholes in Pennsylvania (PDF). Pennsylvania Geological Survey, Educational Series 11.

Langer, W. (2001). Potential Environmental Impacts of Quarrying Stone in Karst - A Literature Review. U.S. Geological Survey, Open-File Report 01-0484.

Lee, C. Y. (1971). Geology, mineralization and some geochemical aspects of the Chenderiang area, Perak, West Malaysia. Unpubl. BsC. Thesis. P 129.

Loke, M. H., & Barker, R. D. (1994). Rapid least-squares inversion of apparent resistivity pseudo-sections. Extended Abstracts of Papers 56thEAGE Meeting Vienna, Austria 6-10 June 1994, p. 1002.

Muhammad, R. F. (2003). The Characteristic and Origin of the Tropical Limestone Karst of the Sungai Perak Basin, Malaysia. Unpubl. PhD, University of Malaya, p. 443.

Muhammad, R. F., & Yeap, E. B. (2002). Estimating Dissolution Rates in Kinta and Lenggong Valleys the Micro Erosion Meter. *Geol Soc Bull., 45*, 26-27.

Newton, J. G. (1987). Development of Sinkholes Resulting From Man's Activities in the Eastern United States. US Geological Survey, Circular 968.

Pierson, B. J. (2009). The limestone hills of the Kinta Valley a part of Malaysia's geological heritage worth preserving. *First Break, 27*, 97-100.

Psomiadis, D., Tsourlos, P., & Albanakis, K. (2008). Electrical resistivity tomography mapping of beach rocks, application to the island of Thassos (N. Greece) Environ. *Earth Sci., 59*, 233-240. http://dx.doi.org/10.1007/s12665-009-0021-9

Reitz, H. M., & Eskridge, D. S. (1977). Construction methods which recognize the mechanics of sinkhole development. In R. R. Dilamarter & S. C. Csallany (Eds.), *Hydrologic problems in karst regions: bowling green* (pp. 432-438). Western Kentucky University, Department of Geology and Geography.

Seng, C. K., & Wong, S. L. (2009). The limestone hills and caves of the Kinta Valley, Malaysian Nature Society, Kuala Lumpur, Malaysia, p. 151.

Sowers, G. F. (1996). Building on sinkholes: Design and construction of foundations in karst terrain (p. 115). American Society of Civil Engineers, New York. http://dx.doi.org/10.1061/9780784401767

Suntharalingam, T. (1984). Quaternary stratigraphy and prospects for tin placer in the Taiping-Lumut area, Perak. *Bull. Geol. Soc.* (pp. 9-32).

Suntharalingam, T. (1968). Upper Palaeozoic stratigraphy of the West of Kampar.

Tan, B. K. (1983). Geology and urban development of Kuala Lumpur, Malaysia, 1986, geological society of Hong Kong, Bullten No.3, oct.1987, pp.127-140.

Tan, B. K. (1987). Some geotechnical aspects of urban development over limestone terrain in Malaysia. Bullten of the international association of engineering geologist, pp. 35, 57, 63.

The, G. H., Mahat, S., & Mohd, S. S. (2001). Characterization, geochemistry and possible usage of the limestone hills in the Kinta Valley area, Perak. In the Proceeding of Geol. Soc. Mal. Annual Geological Conference. Eds. The, G. H., Mohd Shafeea Leman and Ng. T. F. 53-57.

Telford, W. M., Geldart, L. P., & Sheriff, R. E. (1990). *Applied Geophysics* (2nd add). Cambridge University Press, New York. http://dx.doi.org/10.1017/CBO9781139167932

Waltham, A. C., & Fookes, P. G. (2003). Engineering classification of karst ground conditions. *Quarterly Journal of Engineering Geology and Hydrogeology, 36*, 101-118. http://dx.doi.org/10.1144/1470-9236/2002-33

White, W. B. (1988). *Geomorphology and Hydrology of Karst Terrains*. Oxford University Press.

William, E. Doll', Jonathan, E. N., Philip, J. C., Kaufmann, R. D., & Bradley, J. Car-r'(2002). Geophysical Surveys of a Known Karst Feature, Oak Ridge Y-12 Plant, Oak Ridge, Tennessee.

Williams, B. E., & Robinson, R. (1993). Grouting beneath an existing dam founded on karst terrain. In B. F. Beck (Ed.), *Applied karst geology* (pp. 255-258). Proceedings of the 4th conference on sinkholes and the engineering and environmental impacts of karst. AA Balkema, Panama City. Science for Conservation, 198-57.

Williams, P. W. (1993). Environmental change and human impact on karst terrains, an introduction. In P. W. Williams (Ed.), Karst Terrains, environmental changes, human impact. Catena Supplement 25: 1–19.58 Urich - Land use in karst terrain.

Yahia, N. A., Yassin, R. R., & Abdel qadir, S. O. (1992). The results of Applying geophysical techniques in Prospecting and Investigation of Bauxite Ore deposits in subsurface karst terrains / Iraqi western desert, Rep.no.2262,geosurv, Baghdad – Iraq.

Yahia, N. A., Yassin, R. R., & Hijab S. R. (1994). The application of complex geophysical techniques to detecting and locating the Weakness zone and the water seepage in the body of the AL-Tharthar dam , samara town, Salahuddin province / Iraq , geosurv. / Baghdad – Iraq, NI-38-10, SEGSM, 2265.

Yassin R. R., Hj Taib, S., & Muhammad, R. F. (2012). Determine Sinkholes and overburden thicknesses in selected covered carbonate Karst Terrains (Kinta valley), Perak, Malaysia by combining Wenner E.R. Tomography, geological and satellite images techniques, The 8th physics, math and Geosciences conference, in Bangkok –Thailand.

Yassin R. R., Hj Taib, S., & Muhammad, R. F. (2013). Reliability of Wenner ER Tomography and satellite image techniques in recognizing and assessing the geohazard development of subsurface carbonate karst features in selected construction sites in (Kinta valley). Perak, Peninsular Malaysia, The fifth regional conference on Geological Engineering, Kuala Lumpur, Malaysia.ISBN:978-967-0380-23-0.

Yassin, R. R. (2002). evaluates the presence of karstic Bauxitic clay deposits in parts of western desert of Iraq by the application of VLF – electromagnetic and Electrical resistivity techniques, MsC thesis submitted to

Department of Geology, college of science, University of Baghdad– Iraq, p. 293.

Yeap, E. B. (1985). Irregular topography of subsurface carbonate bedrock in Kuala Lumpur area, Malaysia. *The 8th southeast Asia Geotechnical Conference, Kuala Lumpur*, vol. 1, p.12.

Yin, E. H. (1976). New Series Regional geology of Peninsular Malaysia Peninsular Malaysia, 1:63,630 Sheet 94. Kuala Lumpur, Geological Survey of Malaysia.

Zhou, W., Beck, B. F., & Stephenson, J. B. (2000). Reliability of dipole-dipole electrical resistivity tomography for defining depth to bedrock in covered karst terrains.